Supporting Information

Bacteria clustering by polymers induces the expression of quorum sense controlled phenotypes

Leong T. Lui[1], Xuan Xue[2], Cheng Sui[2], Alan Brown[2], David I. Pritchard[2], Nigel Halliday[3], Klaus Winzer[3], Steven M. Howdle[4], Francisco Fernandez-Trillo[2†★], Natalio Krasnogor[5★] and Cameron Alexander[2★]

[1]School of Computer Science, [2]School of Pharmacy, [3]School of Molecular Medical Sciences, Centre for Biomolecular Sciences, [4]School of Chemistry, The University of Nottingham, University Park, Nottingham NG7 2RD, UK. [5] School of Computing Science, Newcastle University, Newcastle NE1 7RU, UK.[†] Present address: School of Chemistry, University of Birmingham, Birmingham B15 2TT, UK

★e-mail: f.fernandez-trillo@bham.ac.uk, natalio.krasnogor@ncl.ac.uk, cameron.alexander@nottingham.ac.uk.

Table of Contents

Materials and methods

Poly(N-(3-(Dimethylamino)propyl)methacrylamide) (**P1**)[1,2] and poly(N-dopamine methacrylamide-co-N-(3-(dimethylamino)propyl)methacrylamide) (**P3**)[3] were synthesized according to protocols described in the literature. Poly(vinyl alcohol) (**P2**) (Mw=13,000-23,000, 87%-89% hydrolyzed) was purchased from Sigma-Aldrich®. *(S)*-4,5-Dihydroxy-2,3-pentadione (**DPD**) was purchased from Ommscientific®. N-(3-oxododecanoyl)-L-homoserine lactone (**OdDHL**), N-butyryl-homoserine lactone (**BHL**) were purchased from NovaBiochem (Nottingham, U.K.). We thank Aditi Pathak for the kind donation of 2-heptyl-3-hydroxy-4(1H)-quinolone, usually termed as Pseudomonas quinolone signal (**PQS**). All other chemicals were purchased from Sigma-Aldrich® or Acros® and used without further purification. All solvents were HPLC grade, purchased from Sigma-Aldrich® or Fisher Scientific®, and used without further purification. We thank Bonnie Bassler (Department of Molecular Biology, Princeton University) for the gift of *Vibrio harveyi* strains MM32 and BB170. We thank Stephen P. Diggle (School of Molecular Medical Sciences, University of Nottingham) for the gift of *Escherichia coli* JM109::pSB1075, *E. coli* JM109::pSB536, and *Pseudomonas aeruginosa* PA01 *pqsA* CTX-*lux::pqsA* strains.

Nuclear Magnetic Resonance (NMR) spectra were recorded on a Bruker 400 MHz spectrometer. Chemical shifts are reported in ppm (δ units) downfield from internal tetramethylsilane (dmso-*d6*) or the -OD signal (D_2O). Cationic Gel Permeation Chromatography (CatGPC) was performed on a Polymer Laboratories GPC 50 with RI detector. Separations were performed on series of Eprogen columns [CatSEC 100, 300 and 1000 columns (250 x 4.6 mm, 5 μm bead size, 100, 300 and 1000 Å pore size respectively) fitted with a matching guard column (CatSEC100, 50 x 4.6 mm). The mobile phase was 0.1% TFA solution (pH 2) containing 100 mM NaCl at a flow rate of 0.5 mL/min. Aqueous Gel Permeation Chromatography (AqGPC) was performed on a Polymer Labs GPC50 Plus fitted with differential refractometer (RI), capillary viscometer (DP) and dual angle laser light-scattering (15° and 90°) detectors. The eluent was Dulbecco's PBS without Ca^{2+} and Mg^{2+}, at 30 °C and a flow rate of 1 mL·min^{-1}. The instrument was fitted with a Polymer Labs aquagel-OH guard column (50 × 7.5 mm, 8 μm) followed by a pair of PL aquagel-OH columns (30 and 40, 300 × 7.5 mm, 8 μm). Molecular weights were calculated based on a standard calibration method using poly(vinylpyridine) (CatGPC) or poly(ethylene glycol) (AqGPC) narrow standards. Bacterial aggregation was determined by laser diffraction using a Coulter LS230 particle size analyser (Beckman Coulter, High Wycombe, UK). A Nikon optical microscope equipped with a camera connected to a personal computer was used for optical microscopy studies. A Leica TCS SP confocal microscope was used for fluorescence microscopy. Luminescence and optical densities were recorded on a Tecan Infinite 200 microplate reader unless otherwise stated. 2-way Anova analysis with multiple comparisons was performed using Graphpad® Prism 6 software.

General protocol for RAFT polymerization

Polymerizations were conducted in round bottom flasks sealed with a rubber septum and parafilm. An NMR spectrum was recorded at the beginning of the experiment. The polymerization solutions were degassed using argon for at least 10 min and transferred to an oil bath preheated to 70 °C. After reaction, the solution was quenched by cooling in ice-water and opening to air, and another NMR spectrum was recorded to enable calculation of degree of conversion. For the removal of the RAFT agent, the reaction was carried out at 80 ºC, and the absence of RAFT agent was confirmed by UV spectroscopy.

- **p(DMAPMAm): poly(N-[3-(dimethylamino)propyl] methacrylamide) (P1)**

N-[3-(dimethylamino)propyl] methacrylamide (**DMAPMAm**) (3.68 g, 21.6 mmol), **CTA** (16.4 mg, 73.1 µmol) and V-501 (2.66 mg, 9.49 µmol) were dissolved in acetate buffer (11.6 mL, 10 mM, pH 5.5) and the final pH re-adjusted to 5 using HCl (1M). The polymerization was carried out overnight (23 h, 92% conversion). **p(DMAPMAm)-RAFT** was purified by precipitating into acetone (2x) and dialysis against water and recovered as a light yellow powder (2.83 g, 74%) after freeze-drying from water (dark, 2 days). **(DMAPMAm)-RAFT** (2.83 g, 49.9 µmol) was then dissolved in H_2O (40.0 mL) and V-501 (495 mg, 1.77 mmol) was added. Reaction was carried out overnight. The title compound **p(DMAPMAm)** was purified by dialysis against NaCl (2 x) and water (2 x) and recovered as a white powder (985 mg, 35%) after freeze-drying from water (dark, 2 days) ^{1}H-NMR (D_2O, 400 MHz) δ (ppm) 4.0-3.1 (m, 4H, CH_2-N DMAPMAm), 2.90 (s, 6H, CH_3-N DMAPMAm), 2.1-1.9 (m, 3H, CH_3 MAm), 1.9-1.6 (m, 2H, CH_2 DMAPMAm), 1.2-0.8 (m, 2H, CH_2 MAm backbone), DP[§]=99, Mn (CatGPC) 28414, PDI (CatGPC) 1.75. DP[§]=296, Mn (CatGPC) 50277, PDI (CatGPC) 2.91.

- **p(DMAm-co-DMAPMAm): poly(N-dopamine methacrylamide-co-N-[3-(dimethylamino)propyl] methacrylamide) (P3)**

DMAm (50.00 mg, 0.226 mmol, 2.47 M) in DMF (0.091 mL), N-[3-(dimethylamino)propyl] methacrylamide (**DMAPMAm**) (0.368 mL, 2.034 mmol), **CTA** (5.52 mg, 0.023 mmol, 0.12 M) in DMF (0.188 mL) and V-501 (3.17 mg, 0.011 mmol, 0.06 M) in DMF (0.189 mL) were prepared separately and then mixed together (to make a final 0.27 M concentration of **DMAm**). The polymerization was carried out overnight. **p(DMAm-co-DMAPMAm)-RAFT** was purified by dialysis against water and recovered as a light brown powder (0.18 g, 45.4%) after freeze-drying from water (dark, 2 days). **p(DMAm-co-DMAPMAm)-RAFT** (148.00 mg, 0.019 mmol, 0.01 M) in H_2O (1.800 mL) and V-501 (150.99 mg, 0.539 mmol, 1.35 M) in ethanol (0.400 mL) were prepared separately and then mixed together (to make a final ratio 1:30 of polymer to initiator). In order to remove the RAFT agent, this mixture was degassed and allowed to react at 80 ºC overnight. The title compound **p(DMAm-co-DMAPMAm)** was purified by dialysis against water and recovered as a light brown powder (0.12 g, 81.1%) after freeze-drying from water (dark, 2 days) ^{1}H-NMR (D_2O/TFA 5:1, 400 MHz) δ (ppm) 7.70-6.69 (m, 3H, Ar-H), 3.65-3.48 (m, 2H, CH_2-N DMAm), 3.45-3.05 (m, 4H, CH_2-N DMAPMAm), 3.05-2.66 (m, >8H, N-CH_2-$C\underline{H_2}$ DMAm + CH_3 DMAP), 2.24-1.55 (m, >5H, CH_3-MAm + HN-CH_2-$C\underline{H_2}$-DMAPMAm), 1.34-0.73 (m, 2H, CH_2-MAm backbone) DP(**DMAm**)=10, DP(**DMAPMAm**)=90, Mn (AqGPC) 6633, PDI (AqGPC) 1.05.

Aggregation Experiment

Bacterial suspensions were prepared as follows: A single colony of *V. harveyi* grown on LB agar plates was used to inoculate 2 mL LB medium containing chloramphenicol (10 µg/ml), and kanamycin (50 µg/ml) in the case of BB170. The bacteria were grown with aeration at 30 ºC overnight. Boron depleted AB medium was then inoculated with this preculture to give a bacterial suspension with an OD_{600} of 1.0. Aliquotes of this culture were then mixed with known volumes of stock solutions of polymers in DPBS buffer. The values of polymer concentration reported for the aggregation experiments correspond to the polymer concentrations in these suspensions.

The ability of the polymers to aggregate bacteria was analysed by measuring, at different time intervals, cluster size in the absence (Figure S1) and presence of polymers (Figure S2 and S3). While the average cluster size in the absence and presence of **P2** remained constant throughout the duration of the experiment (Figure S2 and S3, 1st and 3rd

§ DP = degree of polymerization. Calculated by dividing the number of monomers fed into the reaction by the number of RAFT agents. It should reflect the number of monomer units per polymer

column), cluster size shifted significantly towards higher values in the presence of **P1** and **P3** (Figure S2 and S3, 2nd and 4th column). The morphology of these aggregates was observed by optical microscopy (Figure S4 and S5).

- **Average polymer-bacteria cluster**

Size distributions of bacterial clusters were determined under moderate stirring (default speed 5 setting) to the required concentration as indicated by the in-built display software. Particle size ranges were defined using PSS-Duke standards (Polymer Standard Service, Kromatek Ltd, Dunmow, UK). Particle size distribution was then determined as a function of the particle diffraction using the Coulter software (version 2.11a) and plotted as a function of the percentage of distribution volume.

In a typical experiment, bacterial suspensions, in the absence and presence of polymers were added to a flow cell filled with H_2O (~ 14 mL) to obtain an obscuration of 8-12%. Cluster size was then measured at different time intervals.

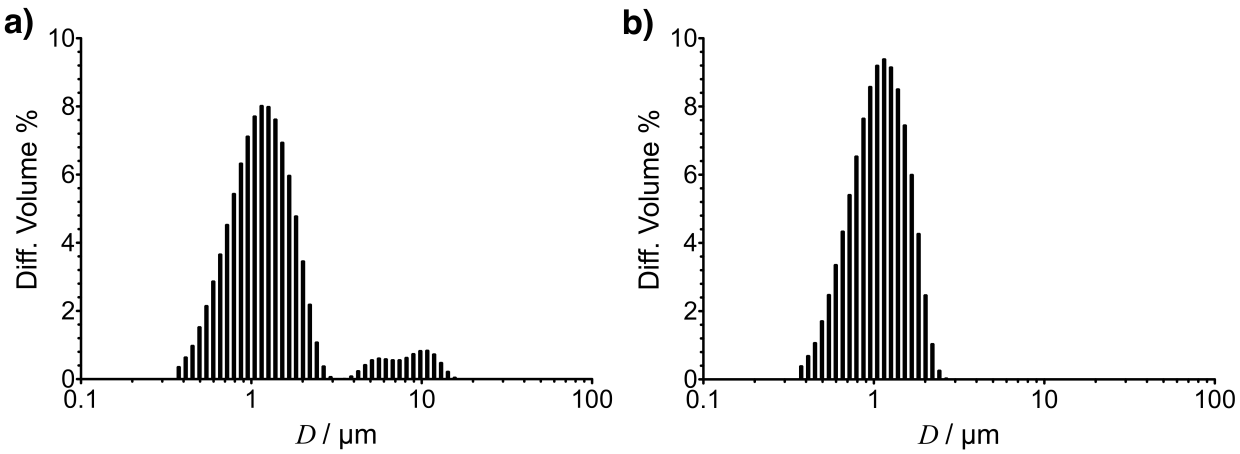

Figure S1: Size distribution of fresh suspensions of *V. harveyi* MM32 (a) and BB170 (b) in AB media in the absence of polymers

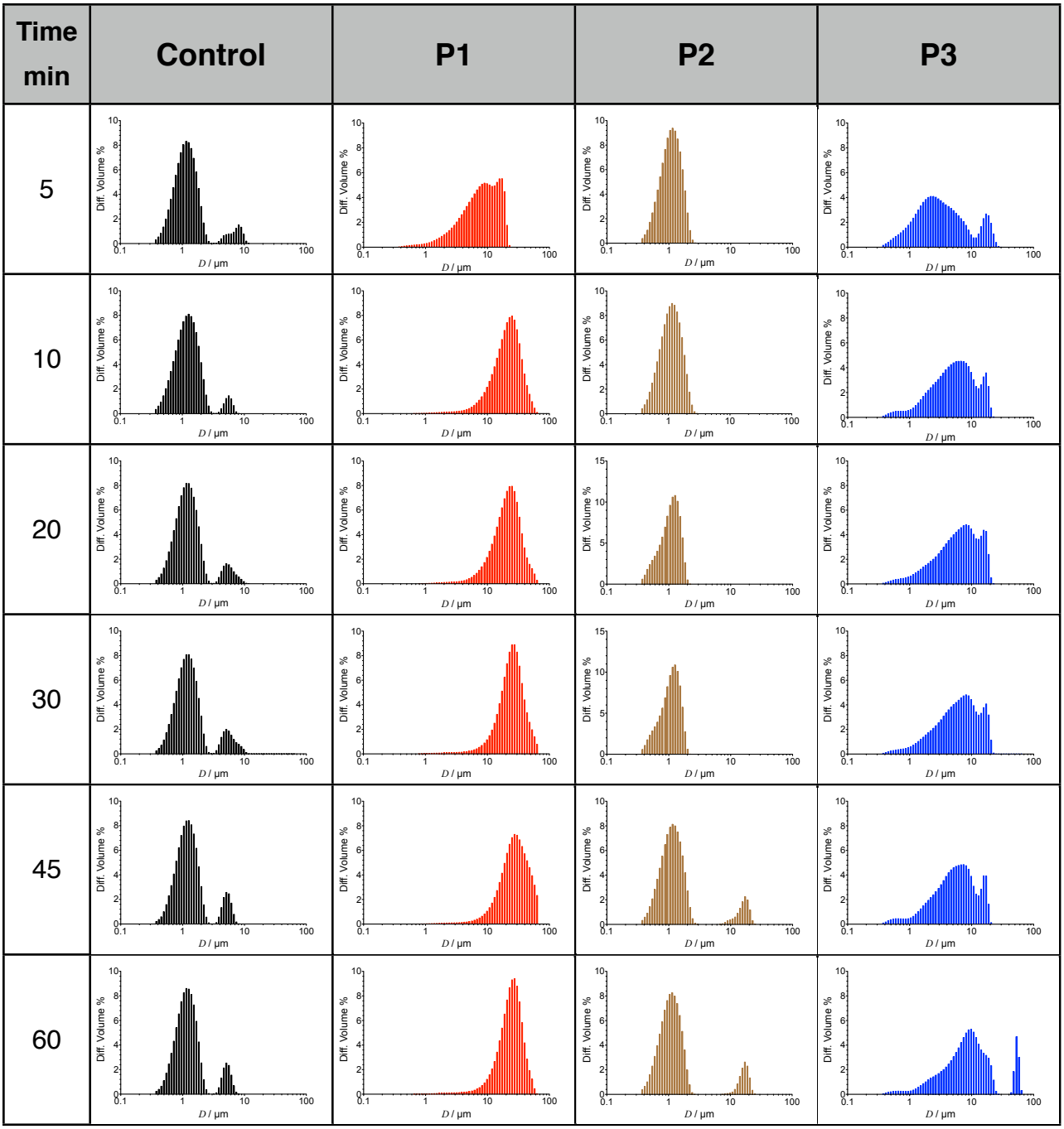

Figure S2: Evolution of size distribution of *V. harveyi* MM32 clusters in suspension in AB media with time in the absence (control) and presence of **P1** (0.25 mg·mL^{-1}), **P2** (0.5 mg·mL^{-1}) and **P3** (0.25 mg·mL^{-1}).

Time min	Control	P1	P2	P3
5	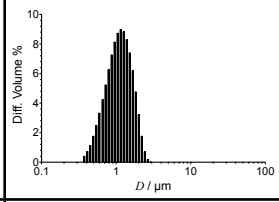	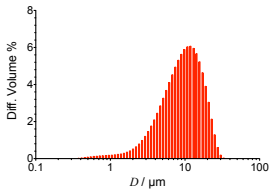	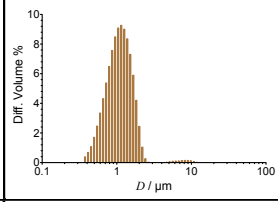	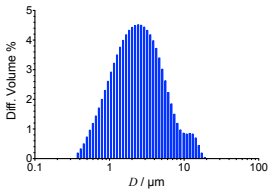
10	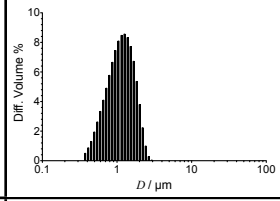	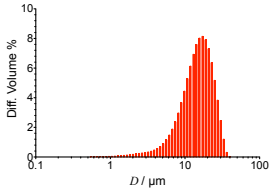	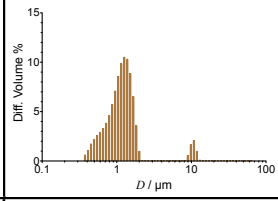	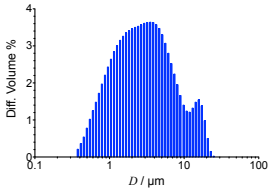
20	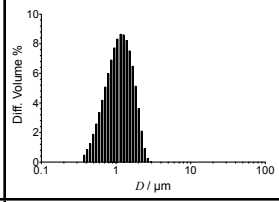	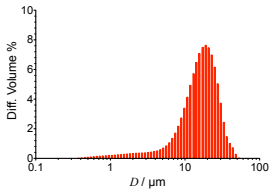	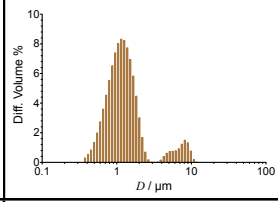	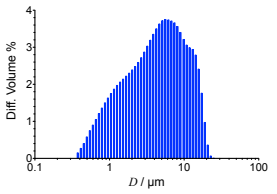
30	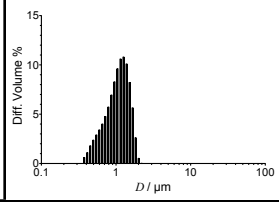	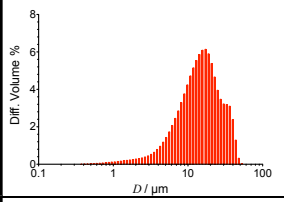	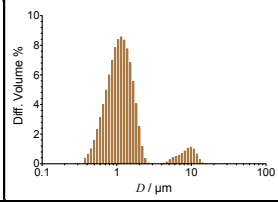	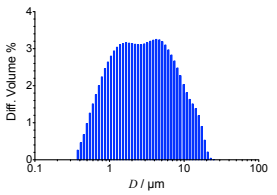
45	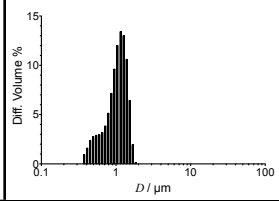	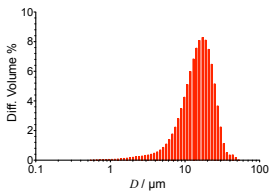	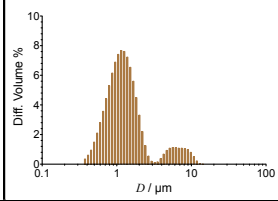	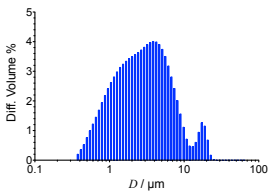
60	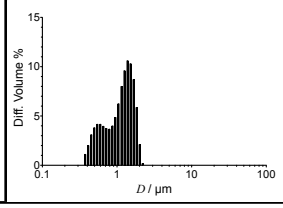	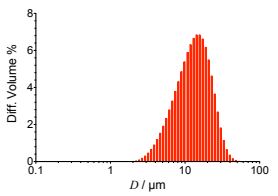	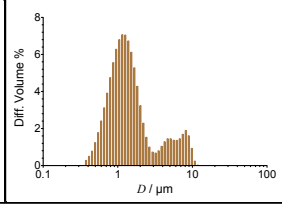	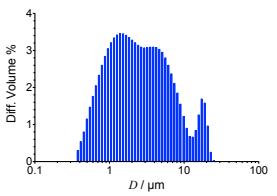

Figure S3: Evolution of size distribution of *V. harveyi* BB170 clusters in suspension in AB media with time in the absence and presence of **P1** (0.25 mg·mL^{-1}), **P2** (0.5 mg·mL^{-1}) and **P3** (0.25 mg·mL^{-1})

- Effect of polymer concentration over aggregation

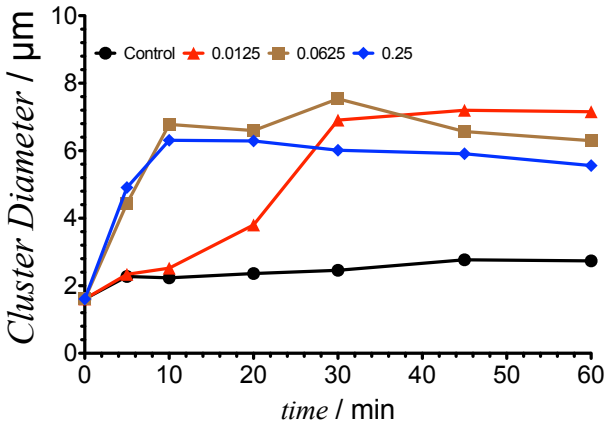

Figure S4: Cluster size as a function of time (min) and polymer concentration (mg·mL^{-1}) for *V. harveyi* MM32 in AB media, dispersed in H_2O, in the absence and presence of **P1**.

- Effect of ionic strength over aggregation

To verify that bacteria clustering in the presence of polymers was driven by electrostatic interactions, the same experiment was conducted using a higher ionic strength buffer (0.15 M NaCl) in the flow cell.

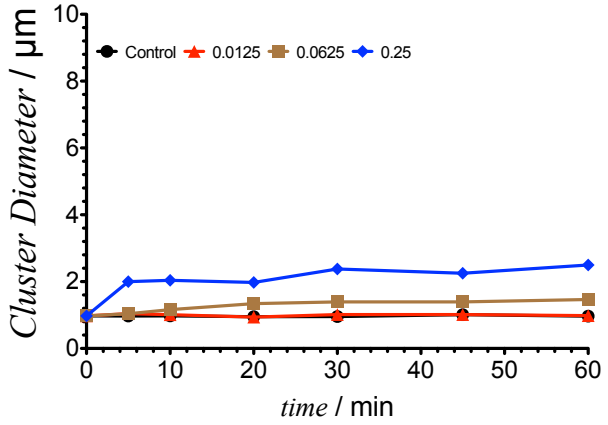

Figure S5: Cluster size as a function of time and polymer concentration (mg·mL^{-1}) for *V. harveyi* MM32 in AB media, dispersed in 0.15 M NaCl, in the absence and presence of **P1**.

- Effect of polymer degree of polymerisation over aggregation

To evaluate the effect DP has over its ability to cluster bacteria, the same experiment was conducted using two independent batches of **P1**.

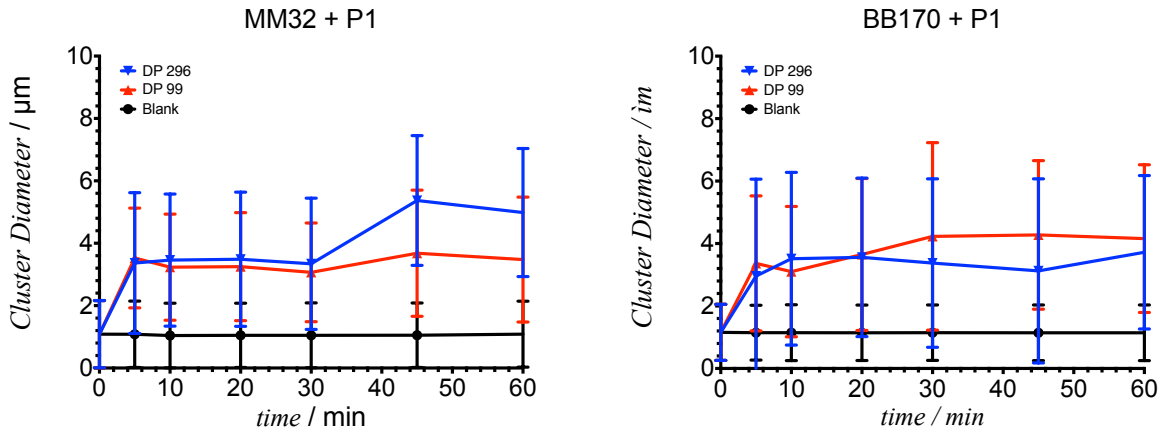

Figure S6: Cluster size as a function of time (min) and polymer DP for *V. harveyi* in AB media, dispersed in H_2O, in the absence and presence of different batches of **P1**.

- **Optical Microscopy**

Aliquots (10µL) of the samples used to measure average cluster size were collected after 60 min, mounted on a glass slide with a cover slip on top and examined with an optical microscope.

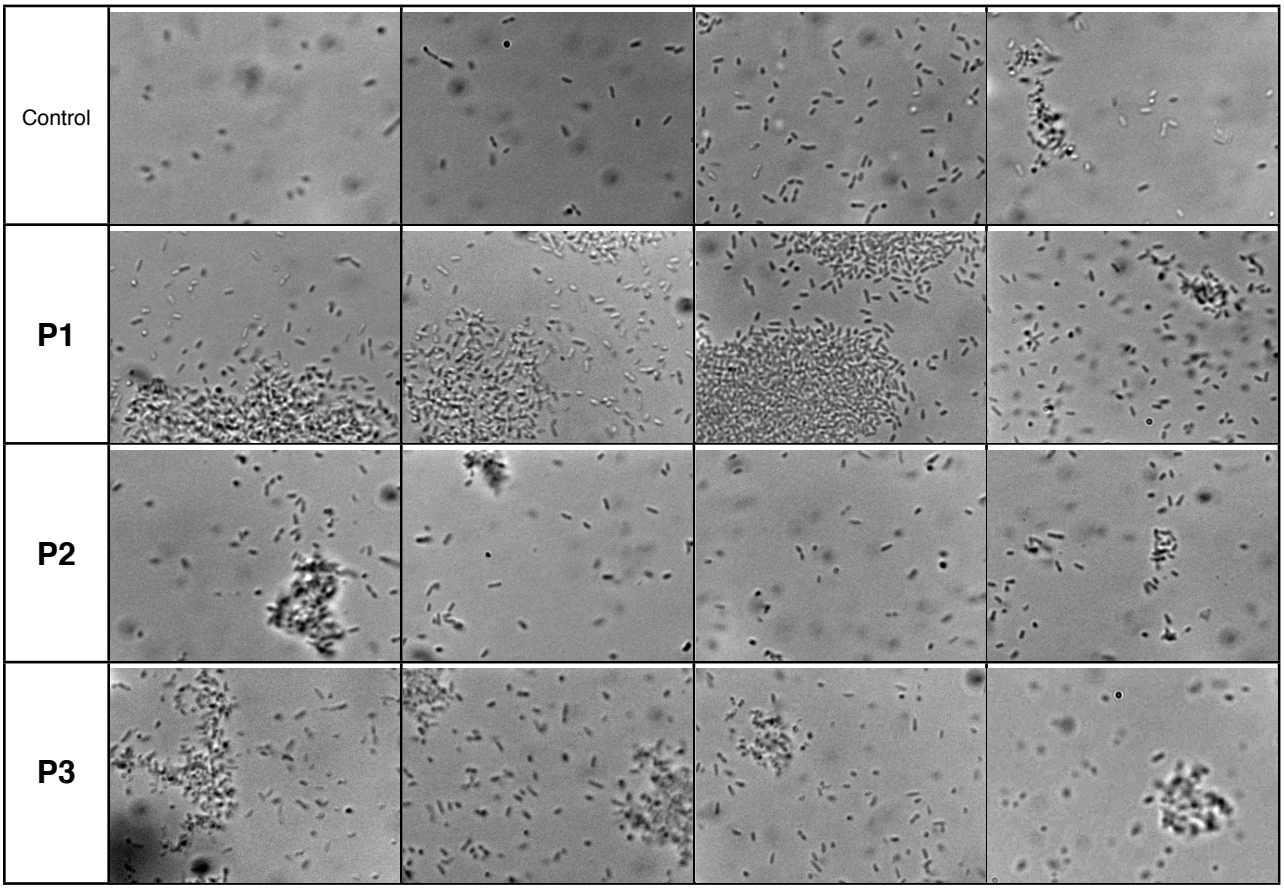

Figure S7: Representative examples of *V. harveyi* MM32-polymer aggregates, as seen by optical microscopy.

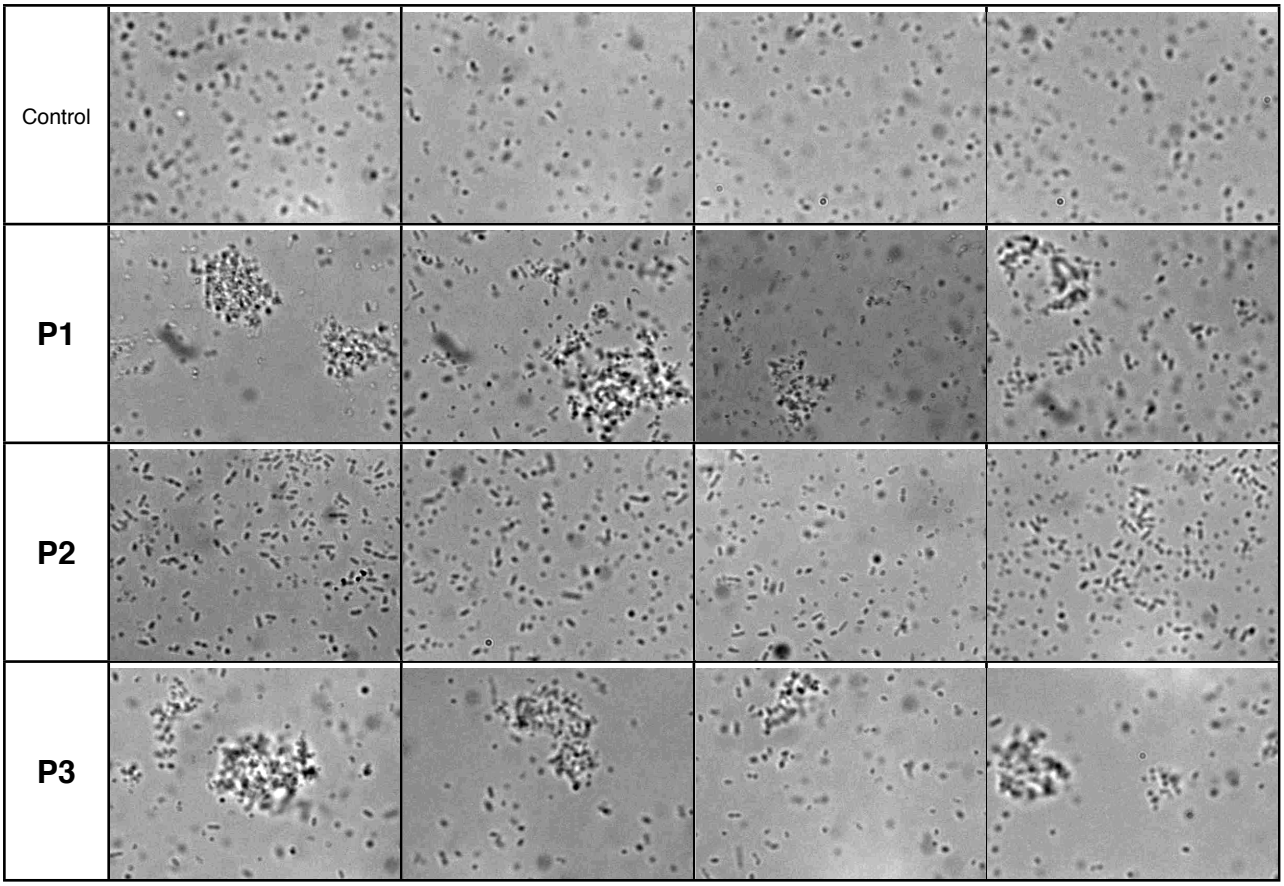

Figure S8: Representative examples of *V. harveyi* BB170-polymer aggregates, as seen by optical microscopy.

Luminescence assay

- ***V. harveyi***

A single colony of *V. harveyi* grown on LB agar plates was used to inoculate 2 mL LB medium containing chloramphenicol (10 µg/ml), and kanamycin (50 µg/ml) in the case of BB170. The bacteria were grown with aeration at 30 ºC overnight. Boron depleted AB medium was then inoculated with this preculture (5000:1). For MM32 boric acid was added to a final concentration of 400 µM, and DPD was added to a final concentration of 22 µM. For BB170 boric acid was added to a final concentration of 22 µM. 180 µL of the inoculated medium were placed in each of the wells of a 96 well plate and combined with 20 µL of the samples to be analysed. Each compound was tested over at least 4 different concentrations. Light production and optical density (600 nm) were recorded at 30 ºC every 30 minutes for at least 10 hours in a 96-well plate, after which time solvent evaporation became a significant issue. The experiments were carried out in triplicate and the plotted curves are derived from the mean value.

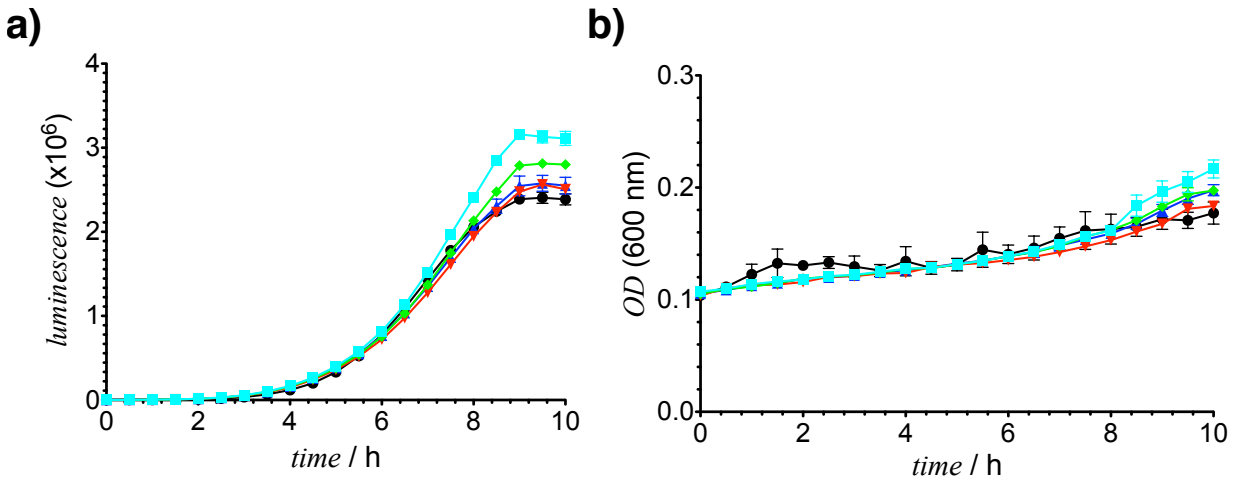

Figure S9: Light production (a) and OD (600 nm) (b), as a function of time for *V. harveyi* MM32 in the absence and presence of **P1** (● No polymer, ▲ 0.05 ▼ 0.125 ◆ 0.25 ■ 0.5 mg·mL^{-1})

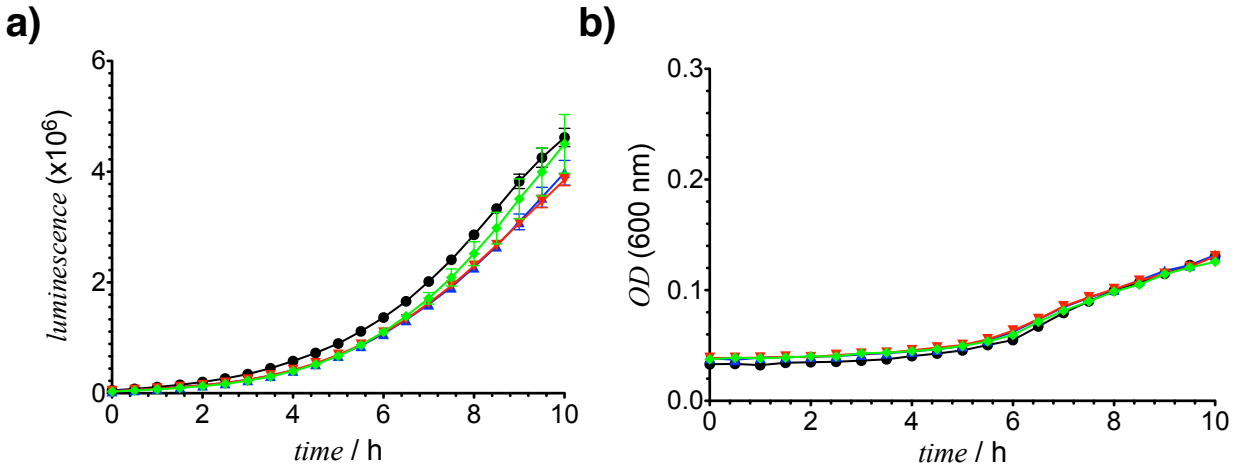

Figure S10: Light production (a) and OD (600 nm) (b), as a function of time for *V. harveyi* MM32 in the absence and presence of **P2** (● No polymer, ▲ 0.5 ▼ 1.0 ◆ 1.5 mg·mL^{-1})

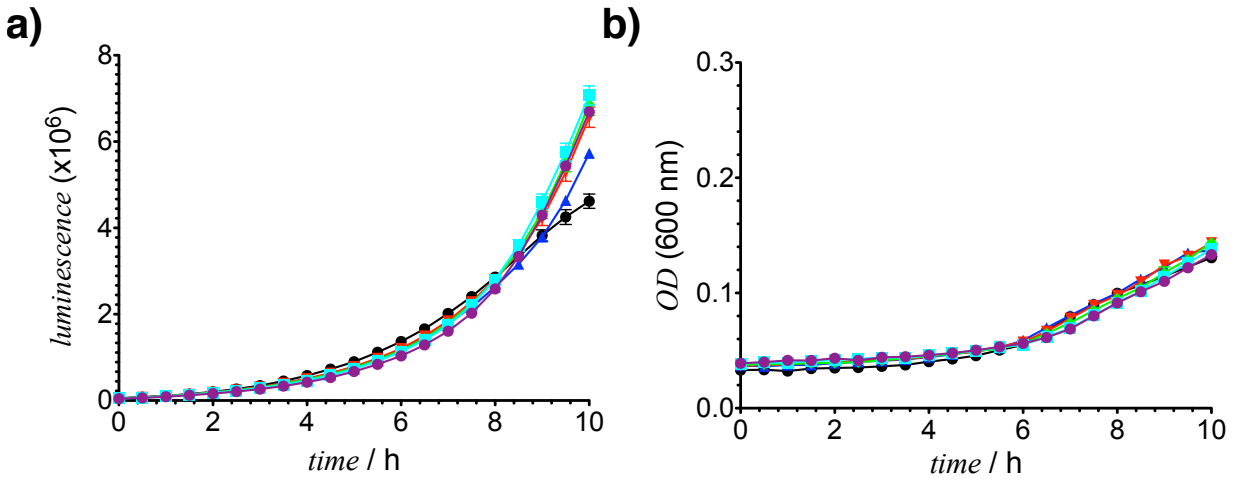

Figure S11: Light production (a) and OD (600 nm) (b), as a function of time for *V. harveyi* MM32 in the absence and presence of **P3** (● No polymer, ▲ 0.025 ▼ 0.05 ◆ 0.125 ■ 0.25 ● 0.5 mg·mL^{-1})

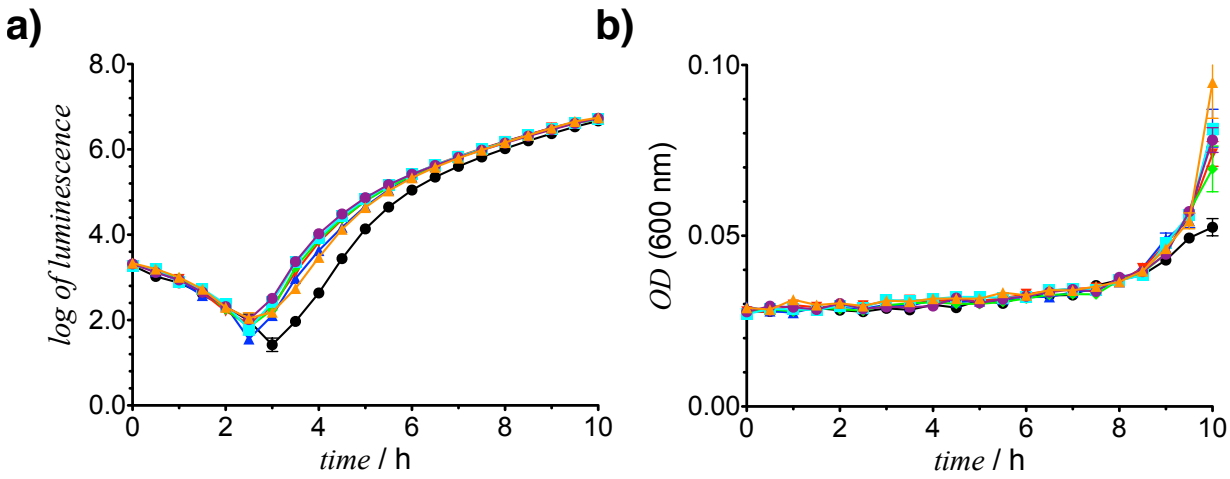

Figure S12: Light production (a) and OD (600 nm) (b), as a function of time for *V. harveyi* BB170 in the absence and presence of **P1**
(● No polymer, ▲ 0.0125 ▼ 0.025 ◆ 0.05 ■ 0.125 ● 0.25 ▲ 0.5 mg·mL^{-1})

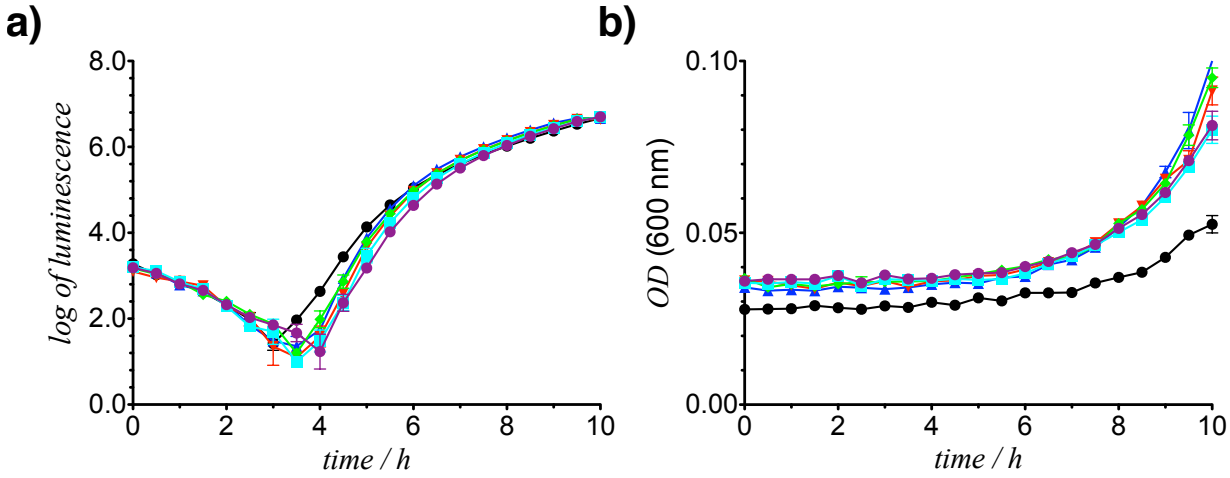

Figure S13: Light production (a) and OD (600 nm) (b), as a function of time for *V. harveyi* BB170 in the absence and presence of **P2** (● No polymer, ▲ 0.01 ▼ 0.05 ◆ 0.1 ■ 0.3 ● 1.5 mg·mL^{-1})

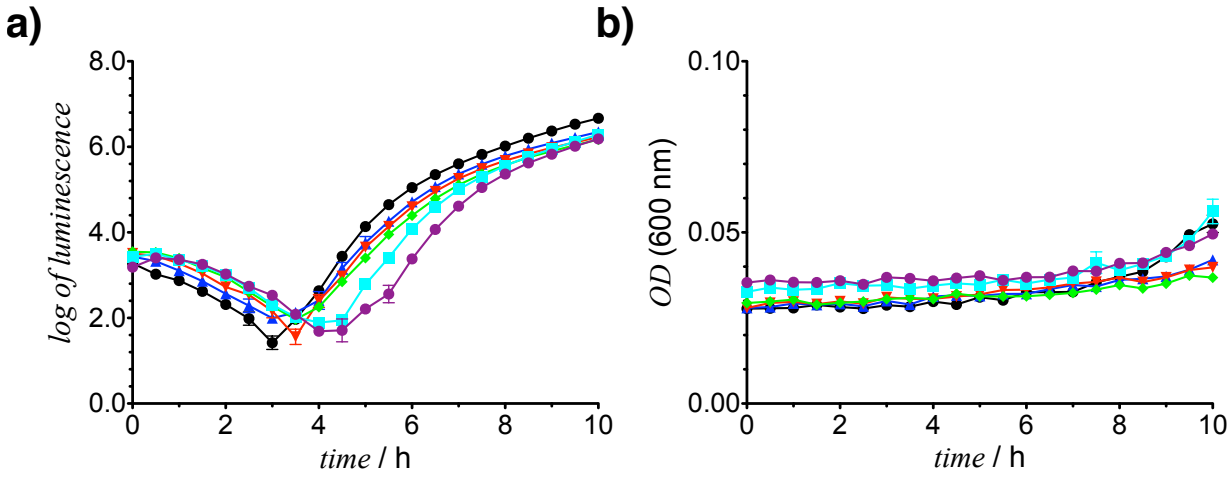

Figure S14: Light production (a) and OD (600 nm) (b), as a function of time for *V. harveyi* BB170 in the absence and presence of **P3**
(● No polymer, ▲ 0.0125 ▼ 0.025 ◆ 0.05 ■ 0.125 ● 0.25 mg·mL^{-1})

- Recovery time

To calculate the recovery time, luminescence during the enhancement phase for the different polymer concentrations was fitted using GraphPad Prism®, and the time to achieve the initial light production in the absence of polymer extrapolated.

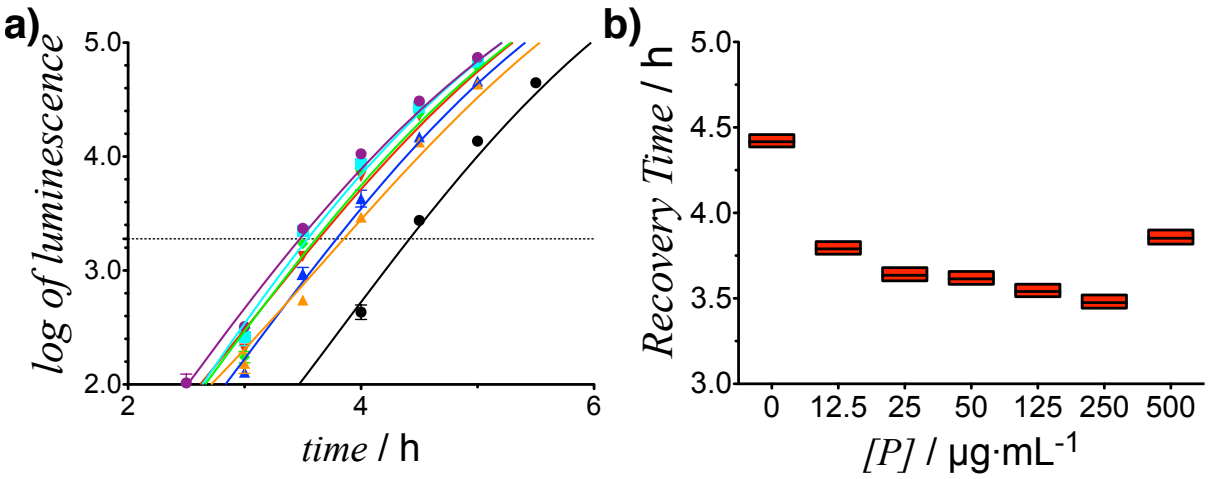

Figure S15: Light production curves (expanded) (a) and recovery time (b) as a function of time for *V. harveyi* BB170 in the absence and presence of **P1** (● No polymer, ▲ 0.0125 ▼ 0.025 ◆ 0.05 ■ 0.125 ● 0.25 ▲ 0.5 mg·mL^{-1})

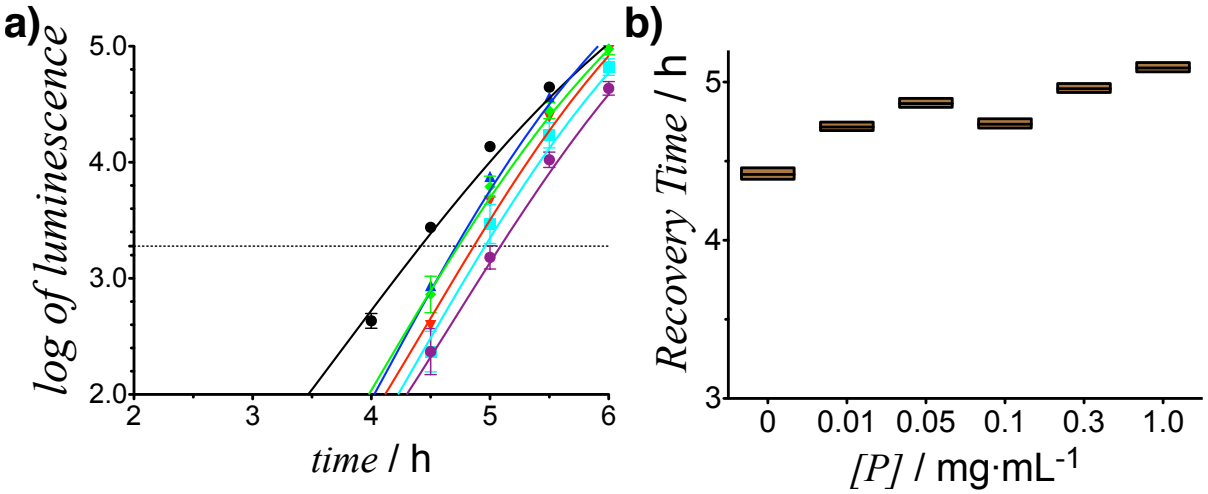

Figure S16: Light production curves (expanded) (a) and recovery time (b) as a function of time for *V. harveyi* BB170 in the absence and presence of **P2**
(● No polymer, ▲ 0.01 ▼ 0.05 ◆ 0.1 ■ 0.3 ● 1.5 mg·mL^{-1})

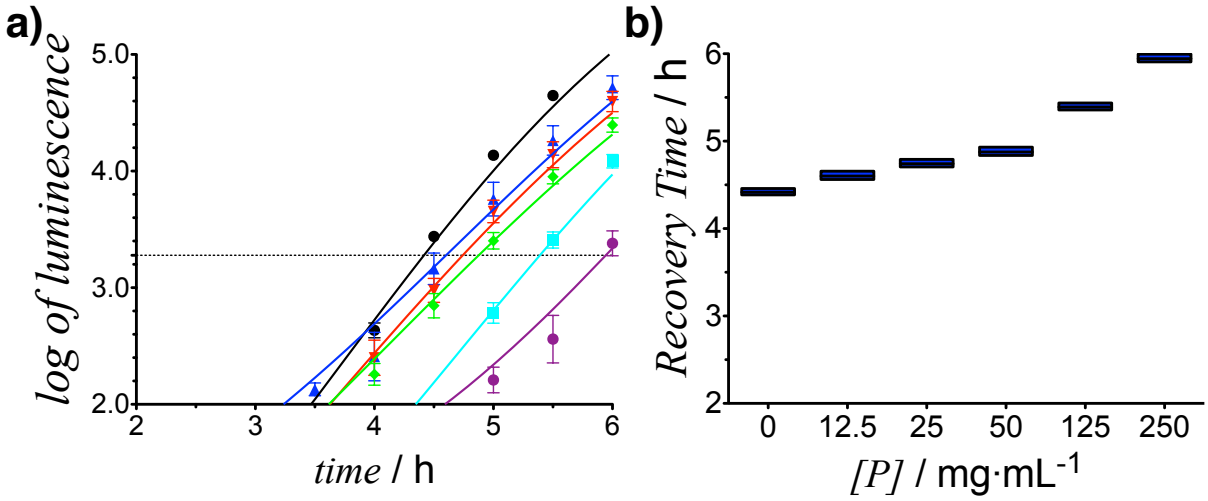

Figure S17: Light production curves (expanded) (a) and recovery time (b) as a function of time for *V. harveyi* BB170 in the absence and presence of **P3**
(● No polymer, ▲ 0.0125 ▼ 0.025 ◆ 0.05 ■ 0.125 ● 0.25 mg·mL^{-1})

- Effect of polymer degree of polymerisation over luminescence

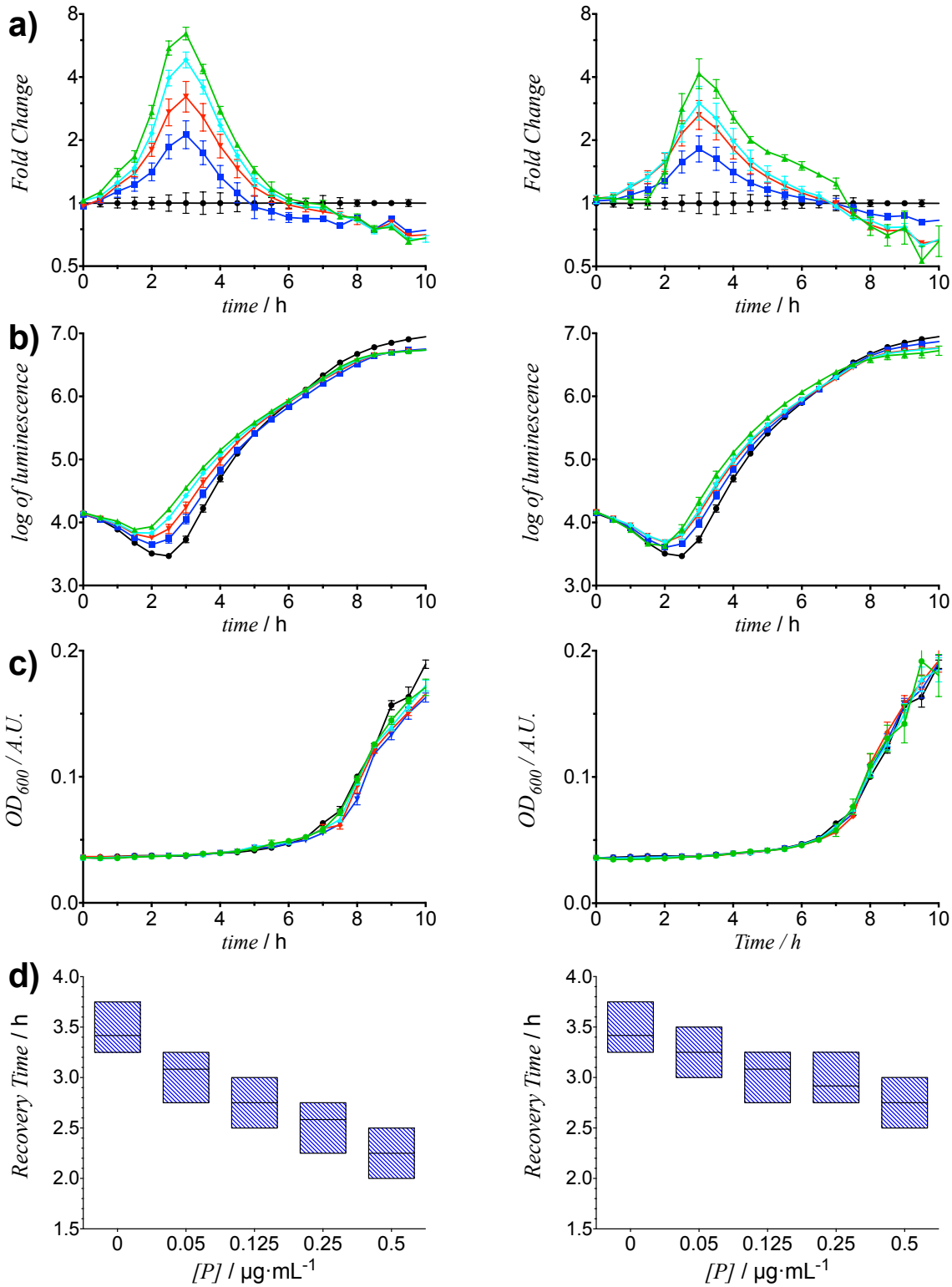

Figure S18: Fold change (a), light production (b), OD (600 nm) (c) and recovery time (d) as a function of time for *V. harveyi* BB170 in the absence and presence of **P1** (DP 99 left, DP 296 right) (● No polymer, ■ 0.05 ▼ 0.125 ◆ 0.25 ▲ 0.5 mg·mL^{-1})

- ***E. coli***

A single colony of *E. coli* JM109 grown on LB agar plates was used to inoculate 5 mL of LB medium supplemented with 5 µL of a 20 mg/mL solution of tetracycline in the case of *E. coli* JM109 containing reporter plasmid pSB1075, or supplemented with 12.5 µL of a 20

mg/mL solution of ampicillin in the case of *E. coli* JM109 containing reporter plasmid pSB536. The bacteria were grown with aeration at 37 °C shaking at 200 r.p.m. LB medium was then inoculated with this preculture (1000:1). 100 µL of the inoculated medium were placed in each of the wells of a 96 well plate and combined with 10 µL of 10 µM solutions of signal molecule (**OdDHL** in the case of *E. coli* JM109 containing reporter plasmid pSB1075, and **BHL** in the case of *E. coli* JM109 containing reporter plasmid pSB536). Different volumes of a polymer stock solution were added and the final volume adjusted to 200 µL with DPBS buffer. Each compound was tested over at least 4 different concentrations. The plate was incubated at 37 ºC and the resulting luminescence measured at 1 h intervals using a Top Count NXT microplate scintillation and luminescence counter (Packard, Meriden, CT, U.S.A.) and optical densities were measured at 1 h intervals using a Dynex MRX microplate reader. The experiments were carried out in triplicate and the plotted curves are derived from the mean value.

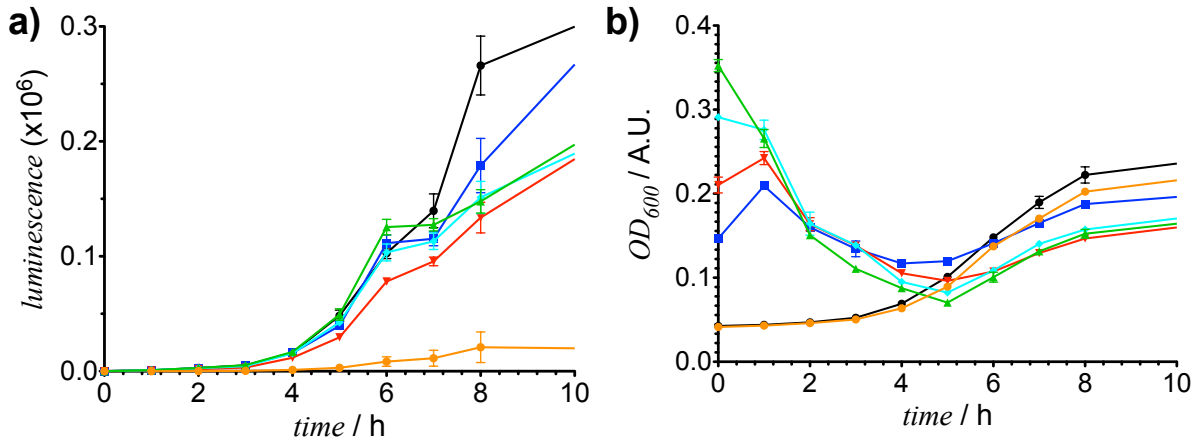

Figure S19: Light production (a) and OD (600 nm) (b), as a function of time for *E. coli* JM109::pSB1075; in the absence and presence of **P1** (● No polymer, ▲ 0.03 ▼ 0.06 ◆ 0.09 ■ 0.125 mg·mL^{-1}, ● No polymer, no signal).

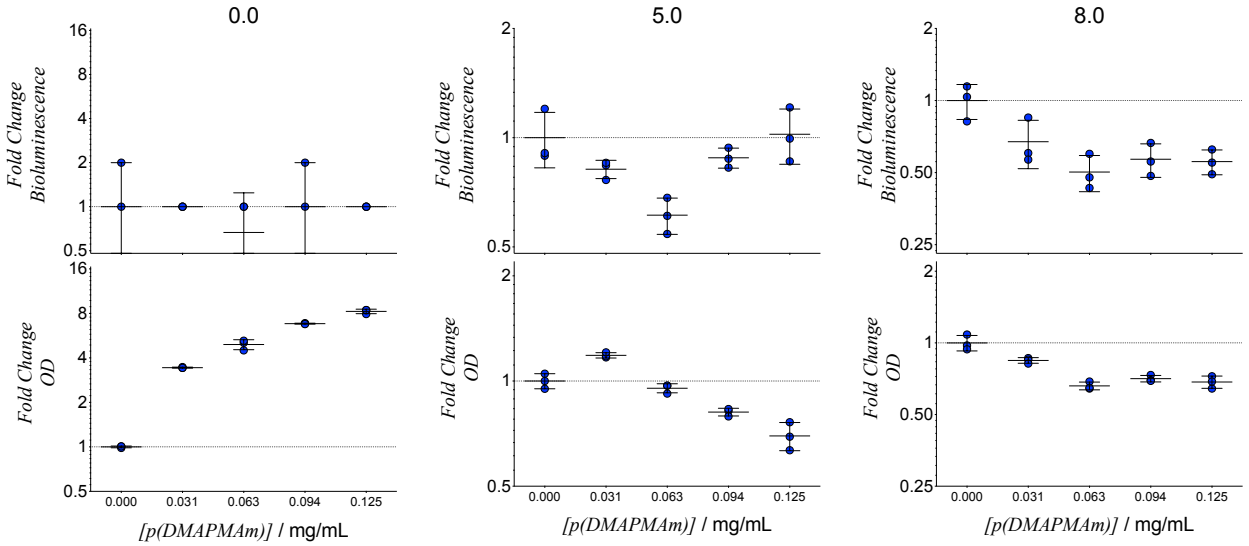

Figure S20: Fold change in light production (top) and OD (bottom) at 0h, 5h and 8 h for *E. coli* JM109::pSB1075; in the absence and presence of **P1**.

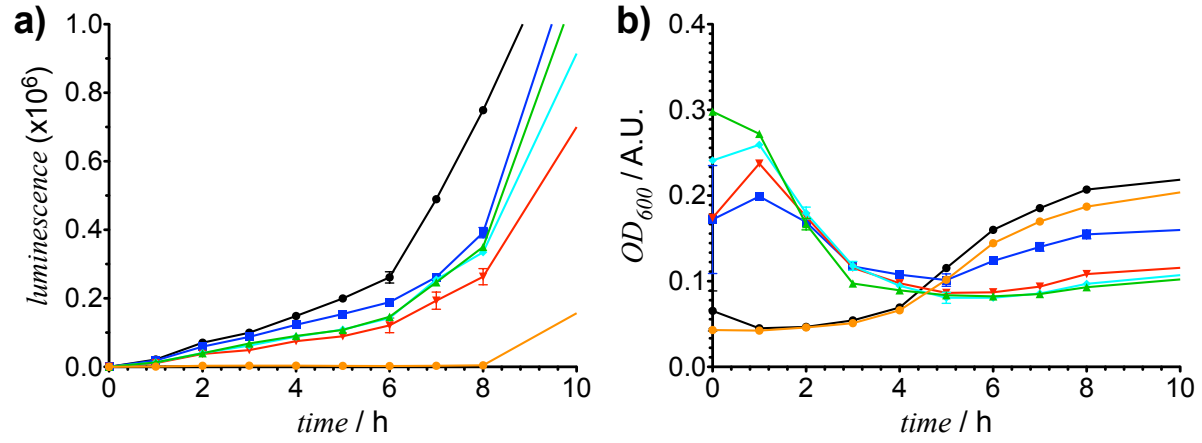

Figure S21: Light production (a) and OD (600 nm) (b), as a function of time for *E. coli* JM109::pSB536; in the absence and presence of **P1** (● No polymer, ▲ 0.03 ▼ 0.06 ◆ 0.09 ■ 0.125 mg·mL^{-1}, ● No polymer, no signal).

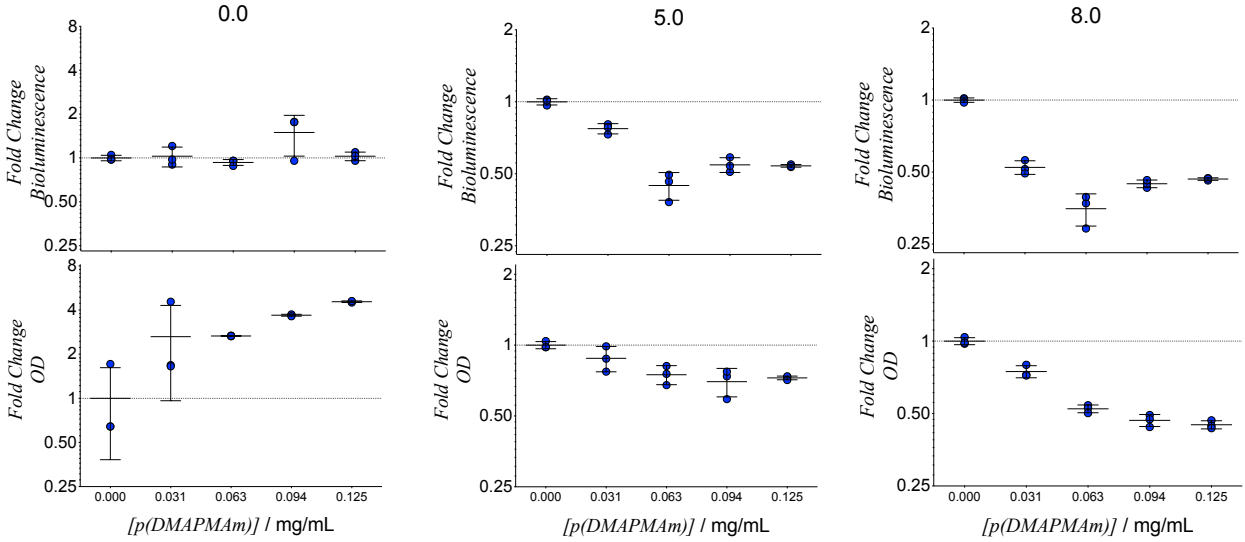

Figure S22: Fold change in light production (top) and OD (bottom) at 0h, 5h and 8 h for *E. coli* JM109::pSB536; in the absence and presence of **P1**.

- ***P. aeruginosa***

A single colony of *P. aeruginosa* grown on LB agar plates was used to inoculate 5 mL of LB medium supplemented with 32 µL of 20 mg/mL of tetracycline. The bacteria were grown with aeration at 37 °C at 200 r.p.m. LB medium was then inoculated with this preculture (1000:1). 100 µL of the inoculated medium were placed in each of the wells of a 96 well plate and combined with 10 µL of 10 µM solutions of signal molecule PQS. Different volumes of a polymer stock solution were added and the final volume adjusted to 200 µL with DPBS buffer. Each compound was tested over at least 4 different concentrations. The plate was incubated at 37 ºC and the resulting luminescence measured at 1 h intervals using a Top Count NXT microplate scintillation and luminescence counter (Packard, Meriden, CT, U.S.A.). The experiments were carried out in triplicate and the plotted curves are derived from the mean value.

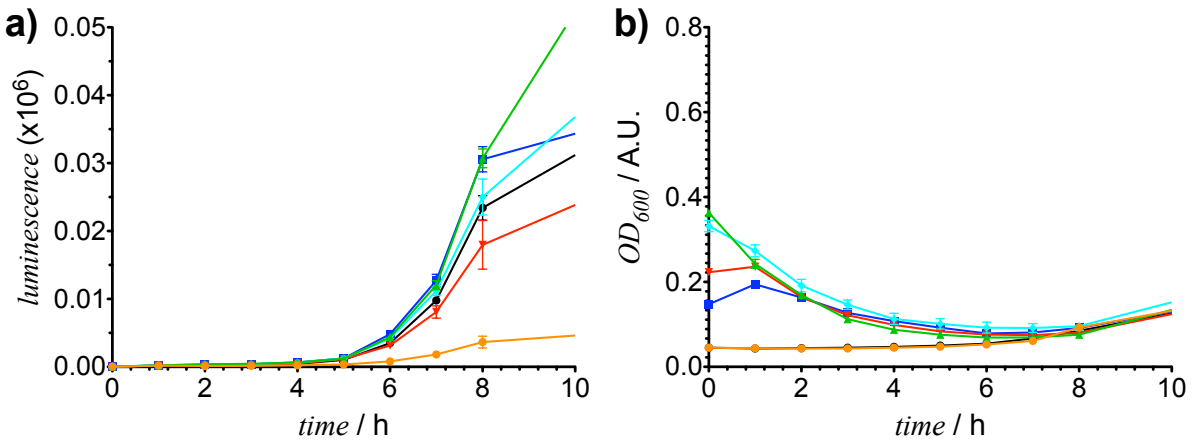

Figure S23: Light production (a) and OD (600 nm) (b), as a function of time for *P. aeruginosa* PA01 *pqsA* CTX-*lux*::*pqsA*; in the absence and presence of **P1** (● No polymer, ▲ 0.03 ▼ 0.06 ◆ 0.09 ■ 0.125 mg·mL^{-1}, ● No polymer, no signal).

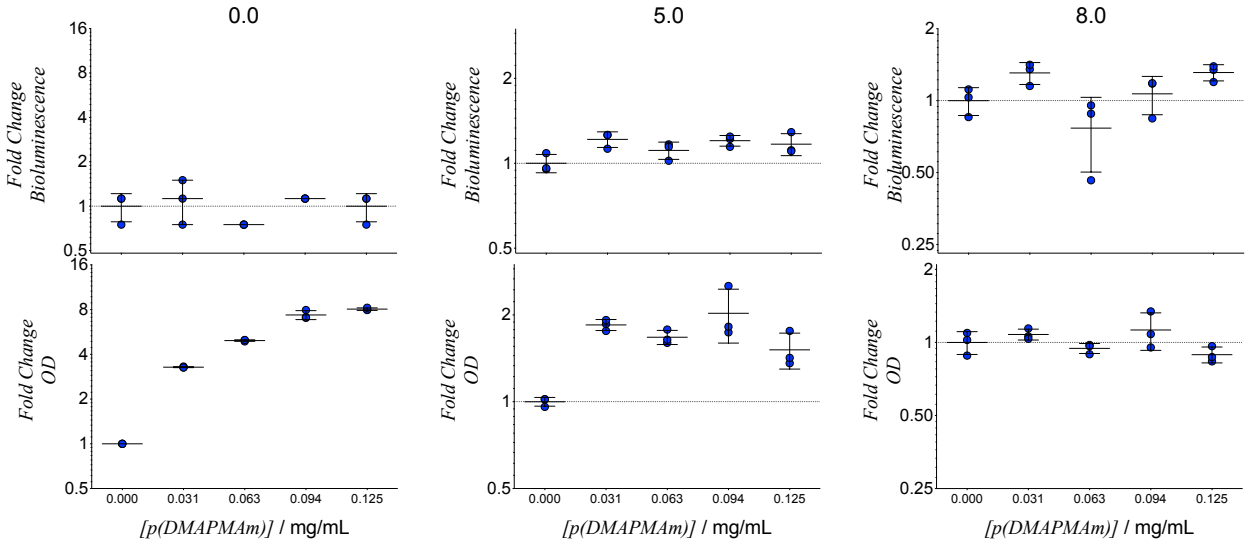

Figure S24: Fold change in light production (top) and OD (bottom) at 0h, 5h and 8 h for *P. aeruginosa* PA01 *pqsA* CTX-*lux*::*pqsA* ; in the absence and presence of **P1**

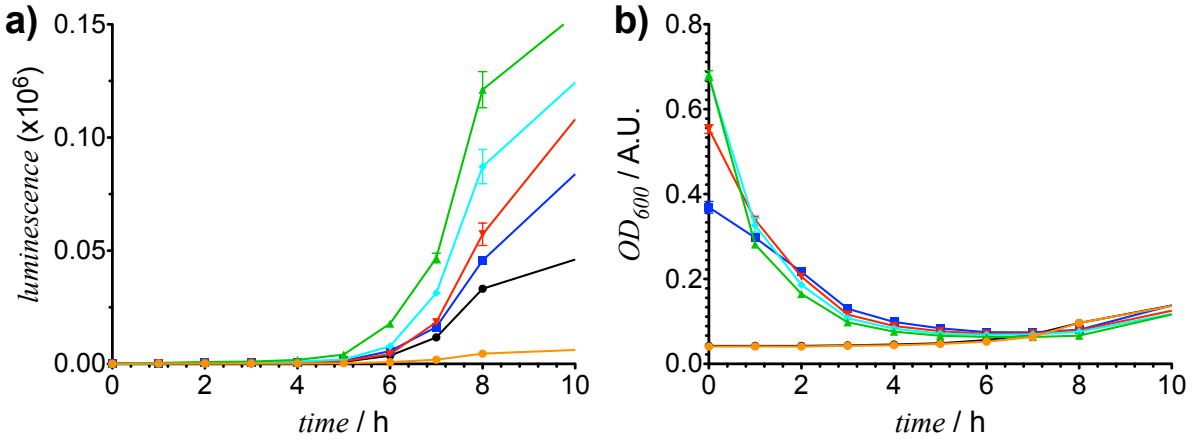

Figure S25: Light production (a) and OD (600 nm) (b), as a function of time for *P. aeruginosa* PA01 *pqsA* CTX-*lux*::*pqsA*; in the absence and presence of **P1** (● No polymer, ▲ 0.125 ▼ 0.25 ◆ 0.375 ■ 0.5 mg·mL^{-1}, ● No polymer, no signal).

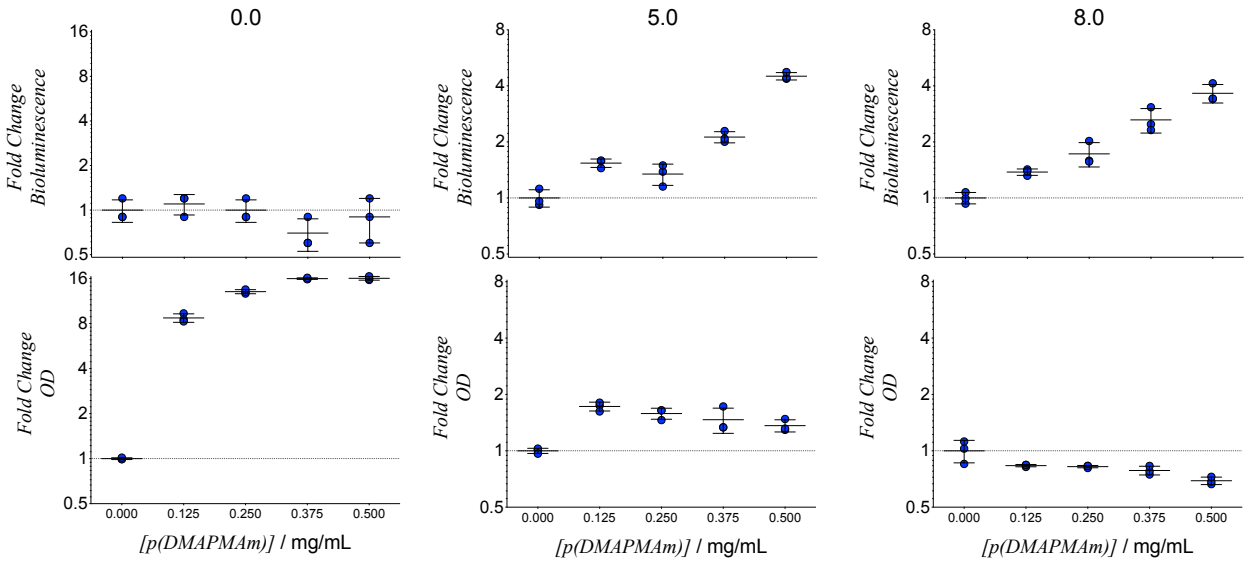

Figure S26: Fold change in light production (top) and OD (bottom) at 0h, 5h and 8 h in for *P. aeruginosa* PA01 *pqsA* CTX-*lux*::*pqsA*; in the absence and presence of **P1**

Viability

- **Live/Dead staining**

Bacteria viability in the absence and presence of polymer was evaluated using a LIVE/DEAD® BacLight Bacterial Viability Kit (REF L7012). In brief, a single colony of *V. harveyi* grown on LB agar plates was used to inoculate 30 mL LB medium. The bacteria were grown with aeration at 30 ºC overnight. 25 mL of this overnight culture were concentrated by centrifugation (10000 g, 10-15 min), and resuspended in 2 mL of 0.85% NaCl buffer. 0.9 mL of this bacterial suspension were then mixed with 0.1 mL of **P1** solution (5 mg/mL) and incubated for 8 h. Untreated bacterial cells were used as positive control, and 0.9 mL of bacterial suspension mixed with 0.1 mL of MeOH were used a negative control. After this time 3 µL of a solution containing equal volumes of green (SYTO 9, 3.34 mM in DMSO) and red (Propidium iodide, 20 mM in DMSO) dye stock solutions were added and this mixture was incubated at room temperature in the dark for 15 minutes. 10 µL of the stained bacterial suspension were trapped between a slide and an 18 mm square coverslip and observed in a fluorescence microscope. At least 18 images were acquired in each case. To quantify viability, red and green levels were measured using ImageJ[4], and their ratio calculated.

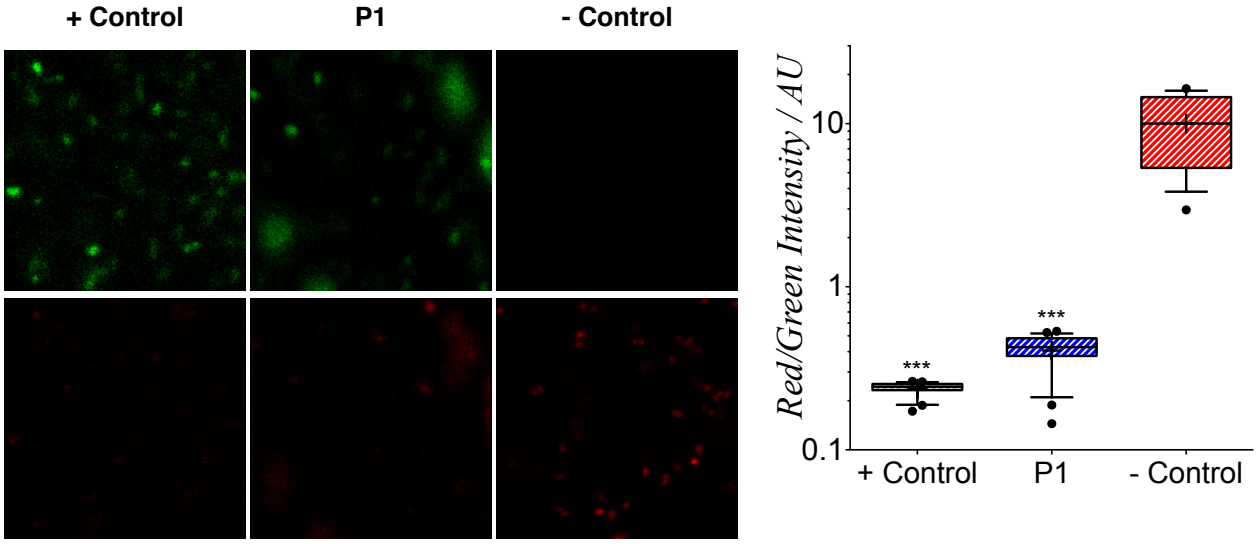

Figure S27: Representative images of green and red channels and ratio of red/green levels for bacterial suspensions in the absence and presence of **P1**. MeOH used as a negative control

Model

- **Physical constrains of the model**

In order to understand the effect that "dual-action" polymers (**P3**) have on QS controlled luminescence in *V. harveyi*, the physical conditions controlling the system have to be defined:

1. The mechanism for signal sequestration based on the competitive formation of borate esters is a reversible process as depicted in equation (1)[5,6];

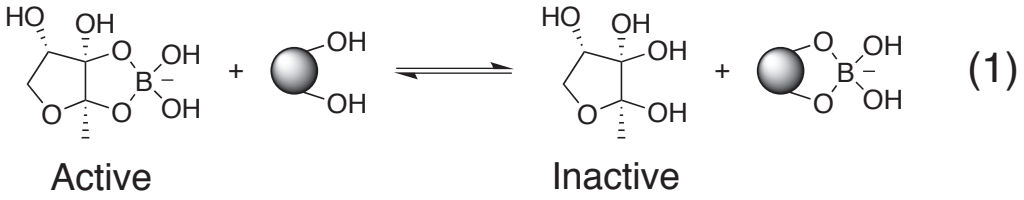

2. Due to the multivalent nature of the interaction, a very small dissociation constant is expected for polymer binding to bacteria[7];
3. AI-2 binding sites in the surface of the polymers should be compromised with time as a consequence of a limited accessibility as polymers cluster at the surface of bacteria;
4. Polymer solutions have a higher viscosity than those of small molecules[8-10]. This increase in viscosity is more pronounced when bacteria and polymers bind to form clusters, limiting the diffusion of small molecules such as AI-2 inside those aggregates;

- **Diffusional modelling**

For each time step, the possible direction for diffusion for each of the objects was evaluated. While it was possible for the smaller objects to move in all 4 directions (except at the boundaries), the bacteria could only diffuse to another lattice site if it was not already occupied by another bacterium. The diffusion rates represented the time taken for one object to move a unit length.

Since there were ~ thousand-fold differences between physical sizes of the bacteria and the smaller molecules (polymers and AI-2), and we expected the bigger entities would affect the diffusion rate of the small entities through entrapment. In the model, the diffusion rates of the smaller molecules were set to be significantly smaller in directions that were blocked by bacteria.

A cluster of bacteria (joined by polymers) was modelled to move collectively, if one bacterium in the cluster was blocked in a specific direction the whole cluster was blocked. As a bacterial-colony diffused towards a specific direction, it was considered to isolate all the small molecules within the lattice sites that were in the same side of the direction of the movement. These features were designed to mimic the local concentration profiles around a bacterial colony assuming it diffused as a single unit.

- **Bacterial division**

Bacteria were modelled to undergo cell division according to a probability distribution $f(t)$, where t = time since last division. Furthermore, when a cell divided, the new cell was randomly assigned to the nearest empty 2×2 lattice space. The "old" cells would thus have exactly the same number of polymers and signal molecules bound to them, whereas the new cell was not bound to any polymers or AI-2 molecules. The probability distribution was set based on growth rates obtained from the luminescence assay experiments.

- **Effect of polymer concentration**

The effect of macro-molecular crowding was incorporated into the model by assuming that when polymers began to aggregate, (increasing the local concentration within a lattice site), there was an effective loss of cell- and signal-binding sites on the polymers inside that lattice site. This was due to hindrance of binding sites on one polymer due to the close proximity of other polymers. In addition, high polymer concentration was considered to lower the diffusion rates of the signal molecules, owing to increased local viscosity and sequential binding events.

- **Model details**

1. The system is represented by a 50×50 two-dimensional grid. There are three types of objects in the model: bacteria (B), polymers (P) and signal molecules (S). Each bacterium occupies a 2×2 space. The positions of the bacteria are defined to be in the vertices of the grids. The polymers and signal molecules are considered to have no significant size. There is no limit on how many signal molecules or polymers can be in a single grid cell. The smaller objects (P and S) can coexist in the same grid cell as the bacteria.
2. The bacteria have two types of binding sites B_P and B_S, for polymers and signal molecules respectively. Similarly, the polymers also have two types of binding sites for bacteria and signal molecules, P_s and P_B. Chemical binding occurs between entities in the same grid cell.
3. The changes in system are implemented by Gillespie Algorithm[11]. There are 3 types of changes from one time step to another in the model, (i) chemical binding/unbinding, (ii) diffusion and (iii) signal production (for the BB170 strain). The rates of the different actions are translated into corresponding propensities (described in the following points). A list of propensity of all the possible changes (chemical reactions and diffusions for all objects) is constructed. The total propensity of the system, A, is given by,

$$A=\sum_{\nu=1}^{\lambda} a_\nu \quad ;$$

where λ is the total number of actions in the system at time t and a_ν is the propensity of action ν. A single action is considered to occur in the time interval (t, $t+\tau$). The action μ is chosen by drawing a random number r_1 from the uniform distribution.

$$\sum_{\nu=1}^{\mu-1} a_\nu < r_1 A \leq \sum_{\nu=1}^{\mu} a_\nu$$

i.e. the successive sum of propensity until μ where the sum equal to or exceed $r_1 A$. In order words, the probability of a particular action to be chosen is given by its own propensity divided by the sum of total propensities of the system. The time step τ is calculated by generating another random number r_2 form the uniform distribution.

$$\tau = \left(\frac{1}{A}\right) \ln\left(\frac{1}{r_2}\right)$$

4. There are three types of chemical bindings in the model:

$$i. \quad P_{B,free} + B_{P,free} \underset{}{\overset{K_{PB}}{\rightleftharpoons}} P_B B_P \; ;$$

$$ii. \quad B_{S,free} + S \overset{K_{BS}}{\rightleftharpoons} B_S S \; ;$$

$$iii. \quad P_{S,free} + S \overset{K_{PS}}{\rightleftharpoons} P_S S \; ;$$

where $P_{B,free}$ is the number of free bacteria binding sites and $P_{S,free}$ the number of free signal binding sites on a polymer, and similarly $B_{P,free}$ the number of free polymer binding sites and $B_{S,free}$ denotes the number of free signal binding sites on the membrane of a bacterium. S is the number of QS signals in a single grid cell. The starting number of bacteria binding sites (P_B) and signal binding sites (P_S) on a polymer are 2 and 5 respectively. The starting number of polymer binding sites (B_P) and signal binding sites (B_S) on a bacterium are 120 and 60 respectively. The starting number of signals (S) is 10000 for MM32 simulation, and 0 for BB170.

The propensity of each reaction is calculated by the number of different reactants multiplied by the reaction rate. For example, for the following chemical reaction between polymers and signal molecules:

$$P_{S,free} + S \underset{k_{PS}-}{\overset{k_{PS}+}{\rightleftharpoons}} P_S S \; ; \; K_{PS} = k_{PS}+ / k_{PS}-$$

the propensity of the binding reactions P_{PS} of the forward reaction is $k_{PS}+ \times P_{S,free} \times S$, where $k_{PS}+$ is the forward reaction rate. Similarly the propensity for the backward reaction is $k_{PS}- \times P_S S$, where $k_{PS}-$ is the backward rate and P_S is the number of polymer-bound signal molecules. The equilibrium constant, K_{PS}, is calculated from the relative propensities. The same algorithms are applied to the other reactions.

Once a polymer is bound to a bacterium, it is then possible to bind to its neighbouring bacteria and form a bacteria cluster as a result.

In our model, K_{BS} was set to be 0.5 (k_{BS}+=0.001, k_{BS}-=0.002.), and K_{PB} and K_{PS} evaluated over a 0.1-10 range (see below for further details).

5. The bacteria take time to produce light as a function of the amount of signal molecules they sense. In the model this is represented by BS_{sense} for the amount of signal molecules bound to the bacteria and $BS_{express}$ for the amount of luciferase genes expressed as a function of signal concentration. In the case of under-expression, i.e. $BS_{sense} > BS_{express}$, new proteins need to be synthesized. For simplicity, the relation between BS_{sense} and $BS_{express}$ is given by,

$$\frac{\partial\left(BS_{express}\right)}{\partial t}=K_{syn}(BS_{sense}\text{-}BS_{express})$$

where K_{syn} is associated with the rate of protein synthesis. For over-expression, i.e. $BS_{sense} < BS_{express}$, it is evaluated by,

$$\frac{\partial\left(BS_{express}\right)}{\partial t}=\text{-}K_{degrad}BS_{express}$$

where K_{degard} represents the rate of protein degradation. K_{syn} is set to be 0.05, and K_{degard} -0.01.

6. The amount of luminescence (lum) produced by each bacterium depends on the number of luciferase genes expressed as follows.

$$lum=Scale\left(1\text{-}\frac{e^{\Delta BS}\text{-}1}{e^{\Delta BS}+1}\right);\ \Delta BS=0.25(BS_c\text{-}BS_{express})$$

BS_c is set to be 15 for BB170 and 38 for MM32. $Scale$ is 2500 for both.

7. The propensity of the diffusion of the entities is the diffusion rate. For example, the propensity for a signal molecule to diffuse to a specific neighbouring grid is D_S, the diffusion rate of signal molecules. The significantly larger size of bacteria would stop the small molecules (signal and polymers) from travelling across and therefore those directions are not available (see below). The D_B and D_P are the diffusion rates of the bacteria and polymers respectfully. The values of the diffusion rates of the objects are inversely proportional to their estimated size, i.e. D_B = 0.0005, D_P = 0.01, D_S = 0.05.

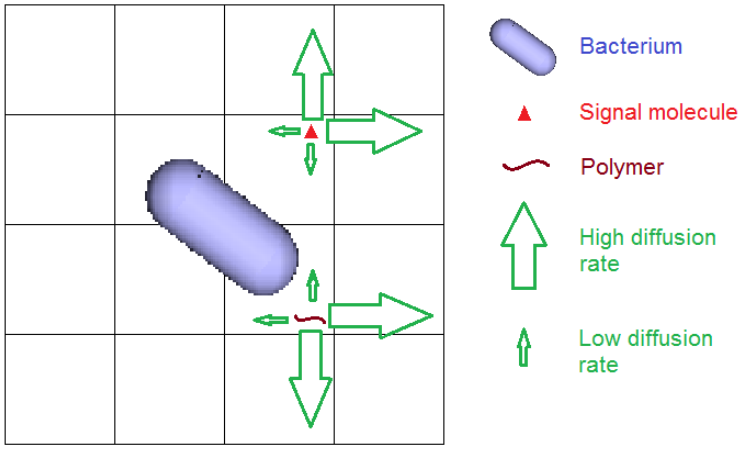

8. The diffusion rate of the signal molecules also depends on the local concentration of the polymers. The dependency, $f(P)$, takes the following form. Therefore, the propensity of signal diffusion becomes $f(P) \times D_S$. λ is set to be 8.

$$f(P)=\frac{1}{2.2}\left(\frac{e^{(\lambda\text{-}[P])}\text{-}1}{e^{(\lambda\text{-}[P])}+1}+1.2\right)$$

9. The bacterial cluster moves as a single unit. The cluster can diffuse to a specific direction if none of its members is blocked in that direction. The diffusion rate of the cluster is modified as D_S/m, where D_S is the diffusion rate of bacteria and m is the number of bacteria in the cluster.

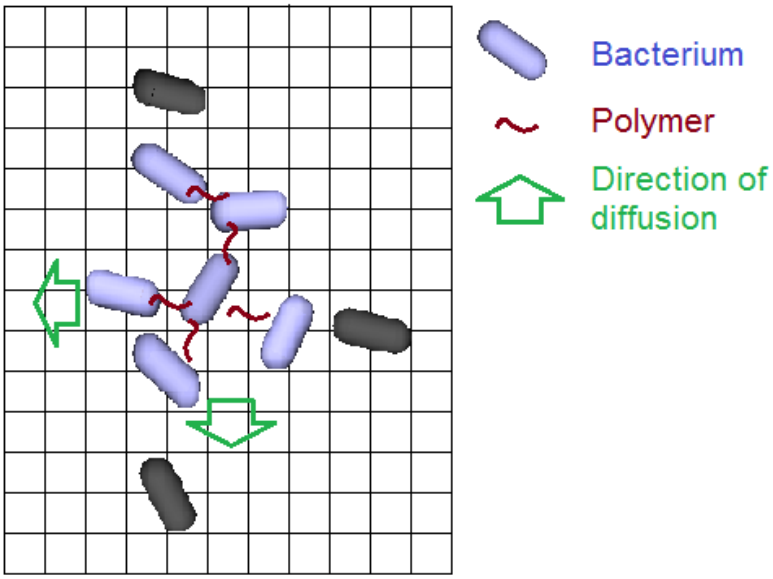

When a bacterial cluster moves, it pushes the smaller chemicals towards the same direction. As a result the concentration profile of the smaller chemicals around the bacterial cluster is maintained.

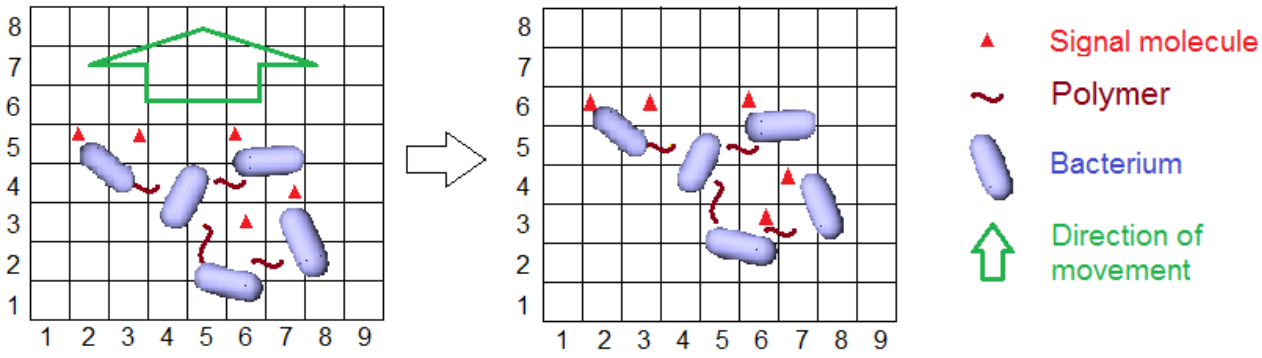

10. The effect of macro-molecular crowding causes a loss of signal binding sites on a polymer due to the close proximity of other polymers when the concentration of polymers is higher than the critical concentration, P_c. Therefore the number of signal binding sites on the polymers becomes

$$P_{S,free}=\begin{cases} P_{S,free}. & P < P_c \\ 0, & P \geq P_c \end{cases}$$

P_c is set to be 10.

11. Bacteria growth is represented by the probability each bacterium has to divide and create a new bacterium. For simplicity this probability distribution was set to be triangular with a mean doubling time (T) of 15000 a.u. and a width of 20000 a.u. The distribution is chosen so that the time evolution of number of bacteria in the system resembles the optical density measured in the luminescence assay experiments. Unless stated otherwise, the starting number of bacteria (B_0) is 25. The maximum number of bacteria in the system is set to be 80 in order to avoid overcrowding.

12. The BB170 strain of the bacteria produce signal molecules at a fixed rate (0.005). When a bacterium produces a signal molecule, the new signal is placed in one of the four grid cells at random.

13. The data presented represents the average of 10 independent runs, using different randomisations, in order to obtain statistically reliable results. The same set of polymers was applied to all simulations unless otherwise stated. Effects were consistent within the 10 simulations. Representative examples of different randomisation for simulated bacteria culture are shown in Figs S23-S25.

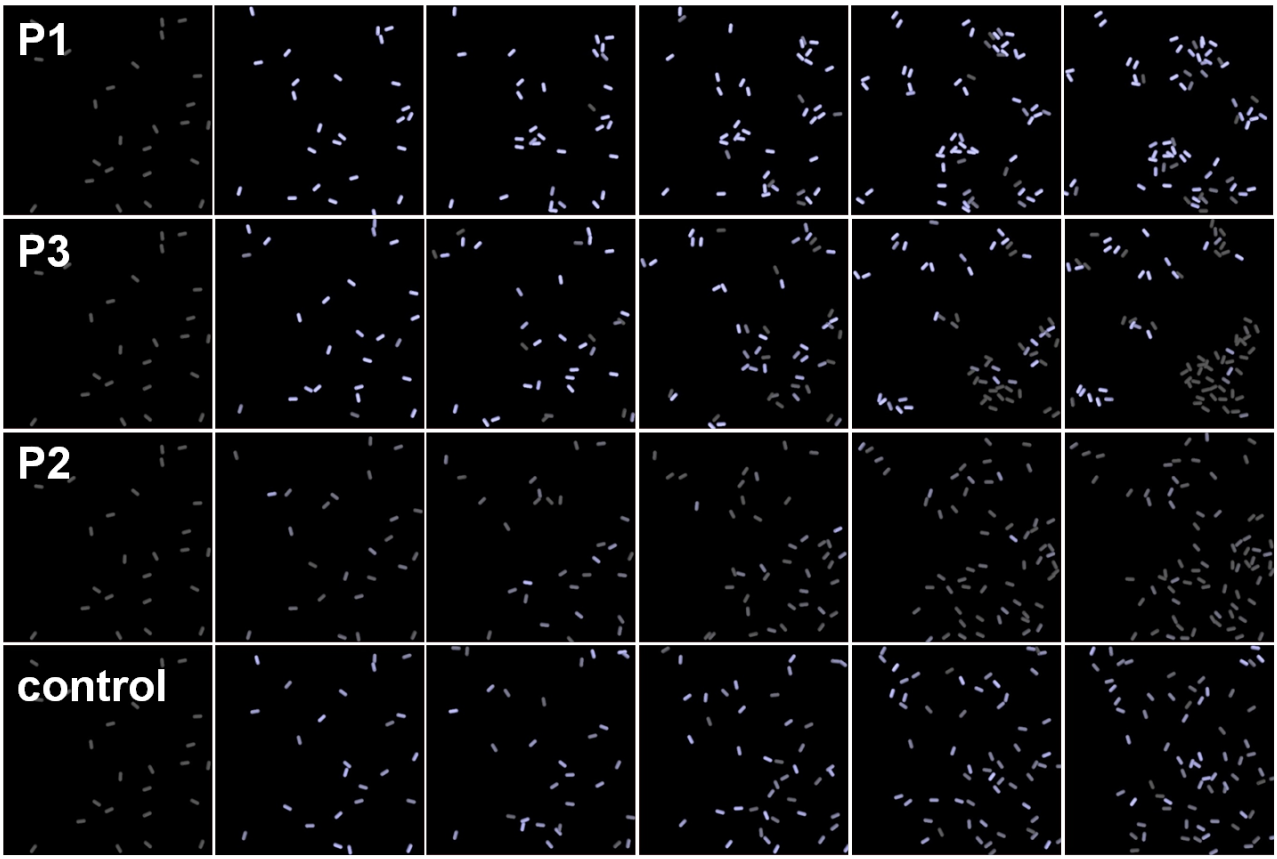

Figure S28: Simultaneous screenshots of simulated bacteria cultures in the absence and presence of polymers (Randomisation 1).

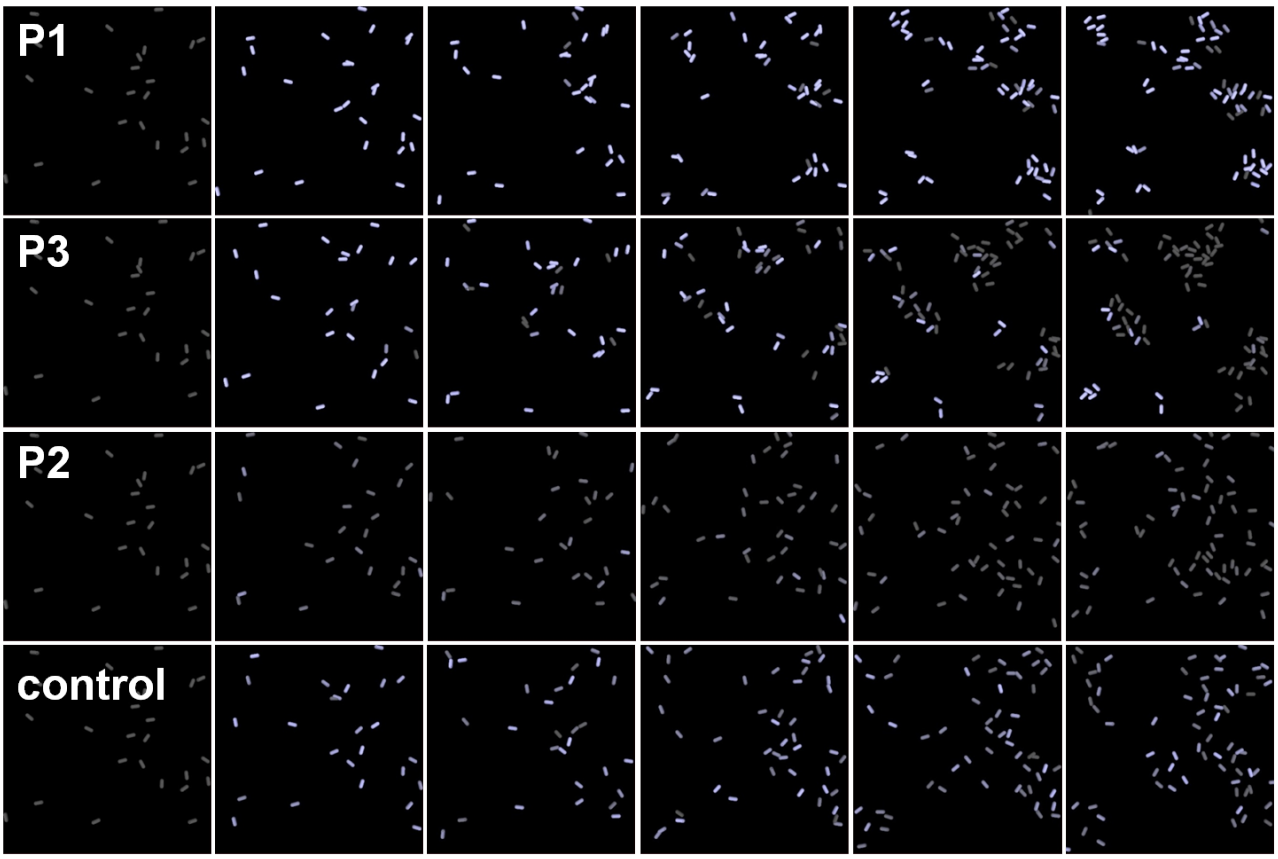

Figure S29: Simultaneous screenshots of simulated bacteria cultures in the absence and presence of polymers (Randomisation 2).

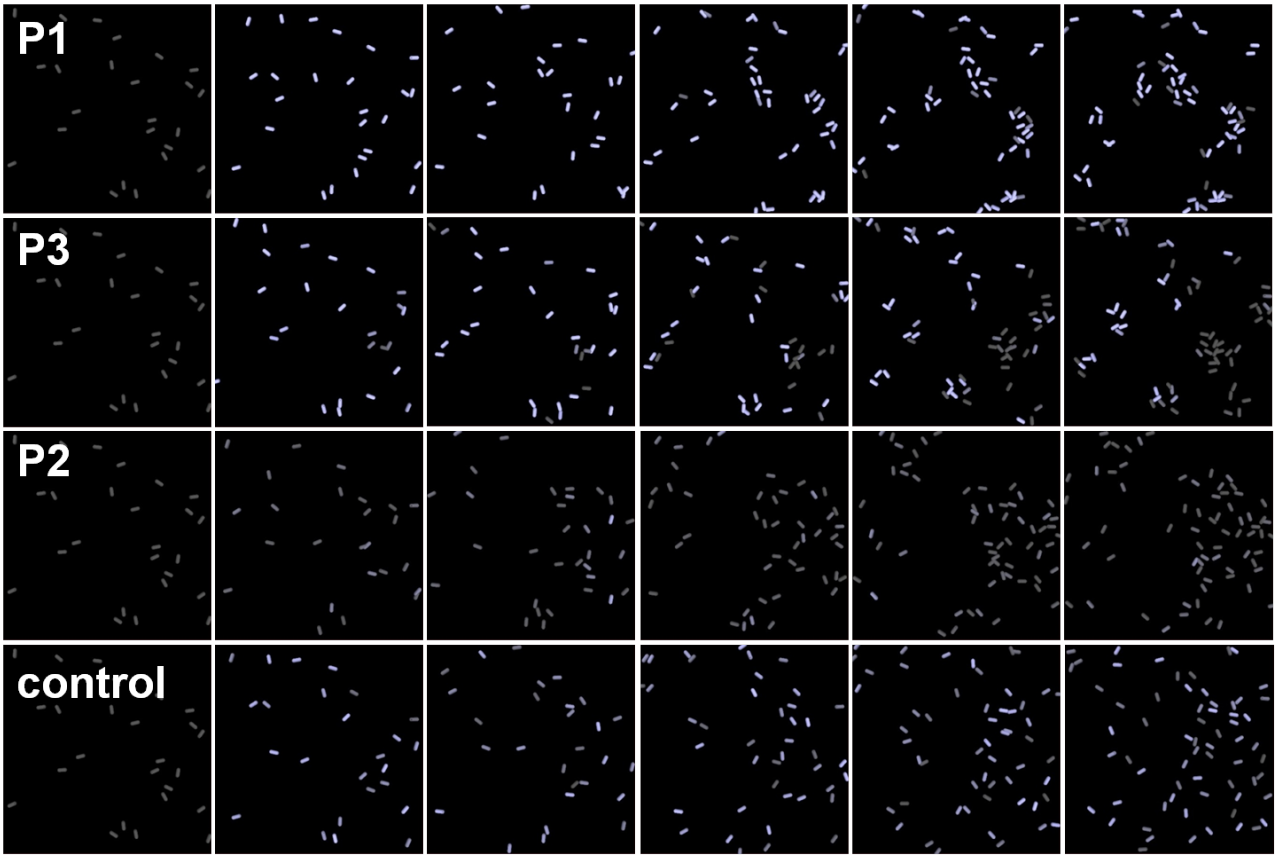

Figure S30: Simultaneous screenshots of simulated bacteria cultures in the absence and presence of polymers (Randomisation 3).

Modelled luminescence

For all experiments, the following parameters were used:

1. [P] was evaluated over a 0-7000 a.u. range, with 1000 a.u. intervals. The color code chosen is as follows: — No polymer — 1000 — 2000 — 3000 — 4000 — 5000 — 6000 — 70000 a.u. This has been omitted from the main text for clarity and the increase in concentration highlighted with an arrow.
2. Time was evaluated over a 0-30000 a.u. range, with 100 a.u. intervals.
3. Affinities for those polymers reported in the main text are: **P1** ⇒ K_{PB} = 5, K_{PS} = 0 a.u.; **P2** ⇒ K_{PB} = 0, K_{PS} = 0.1 a.u.; and **P3** ⇒ K_{PB} = 5, K_{PS} = 10 a.u.

- **Dual-action polymers with different affinities for bacteria and signal.**

The effect polymer affinity for bacteria (K_{PB}) and signals (K_{PS}) has on luminescence expression was investigated using "dual-action" polymers **P3**. Affinities were evaluated over a 0.1-10 a.u. range, as follows: 0.1, 0.5, 1, 5, 10 a.u. A total of 25 simulations were performed. Time = 5000, 15000 and 30000 a.u. were selected as representative early, mid and late time respectively to be plotted in the main text. 3D plots were produced using MATLAB® R2012a. Selected examples of luminescence vs time, and fold change vs time for MM32 are:

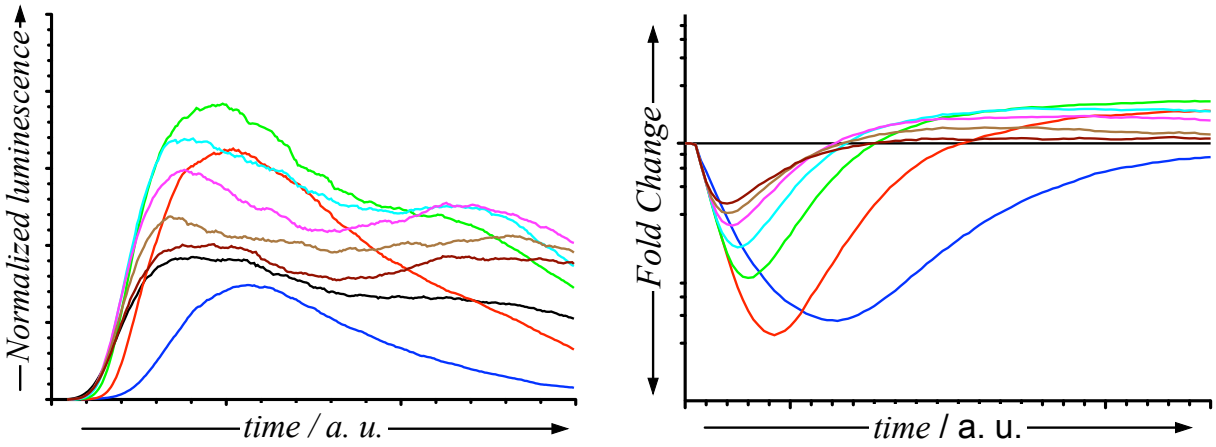

Figure S31: Predicted light production as a function of time for *V. harveyi* MM32 in the absence and presence of **P3** K_{PS} = 10, K_{PB} = 10 a.u. [P] = (— No polymer — 1000 — 2000 — 3000 — 4000 — 5000 — 6000 — 70000 a.u.), time = 0-3000 a.u.

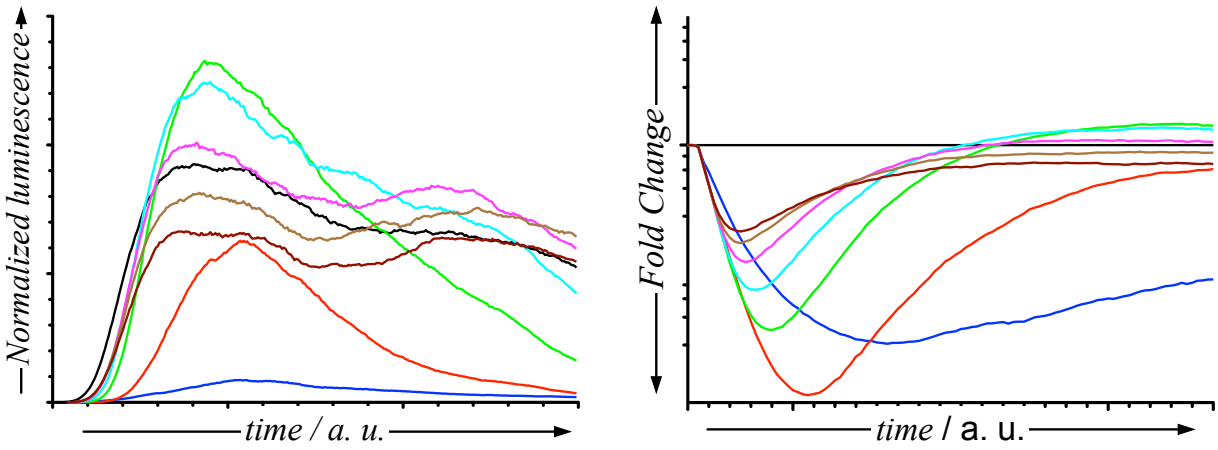

Figure S32: Predicted light production as a function of time for *V. harveyi* MM32 in the absence and presence of **P3** K_{PS} = 10, K_{PB} = 1 a.u. [P] = (— No polymer — 1000 — 2000 — 3000 — 4000 — 5000 — 6000 — 70000 a.u.), time = 0-3000 a.u.

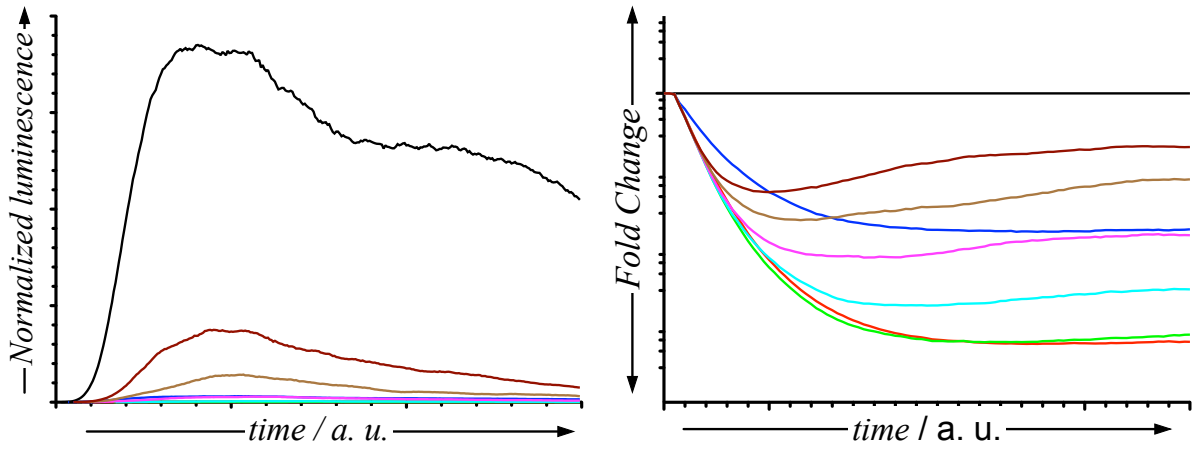

Figure S33: Predicted light production as a function of time for *V. harveyi* MM32 in the absence and presence of **P3** K_{PS} = 10, K_{PB} = 0.1 a.u. [P] = (— No polymer — 1000 — 2000 — 3000 — 4000 — 5000 — 6000 — 70000 a.u.), time = 0-3000 a.u.

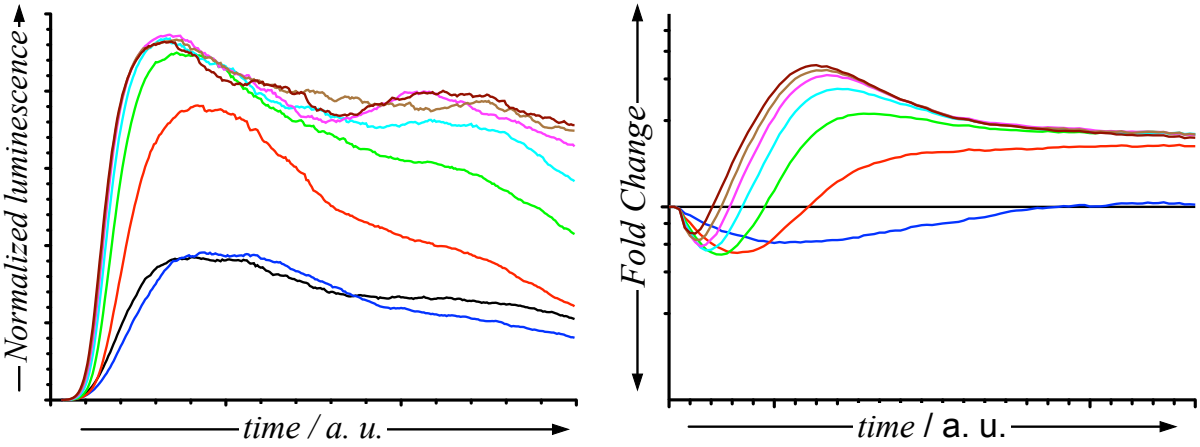

Figure S34: Predicted light production as a function of time for *V. harveyi* MM32 in the absence and presence of **P3** K_{PS} = 1, K_{PB} = 10 a.u. [P] = (— No polymer — 1000 — 2000 — 3000 — 4000 — 5000 — 6000 — 70000 a.u.), time = 0-3000 a.u.

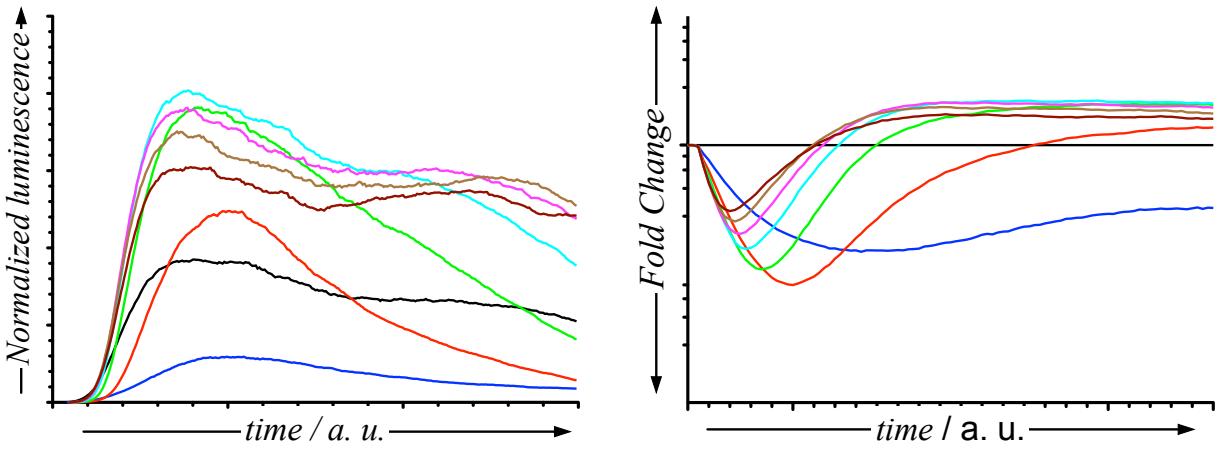

Figure S35: Predicted light production as a function of time for *V. harveyi* MM32 in the absence and presence of **P3** K_{PS} = 1, K_{PB} = 1 a.u. [P] = (— No polymer — 1000 — 2000 — 3000 — 4000 — 5000 — 6000 — 70000 a.u.), time = 0-3000 a.u.

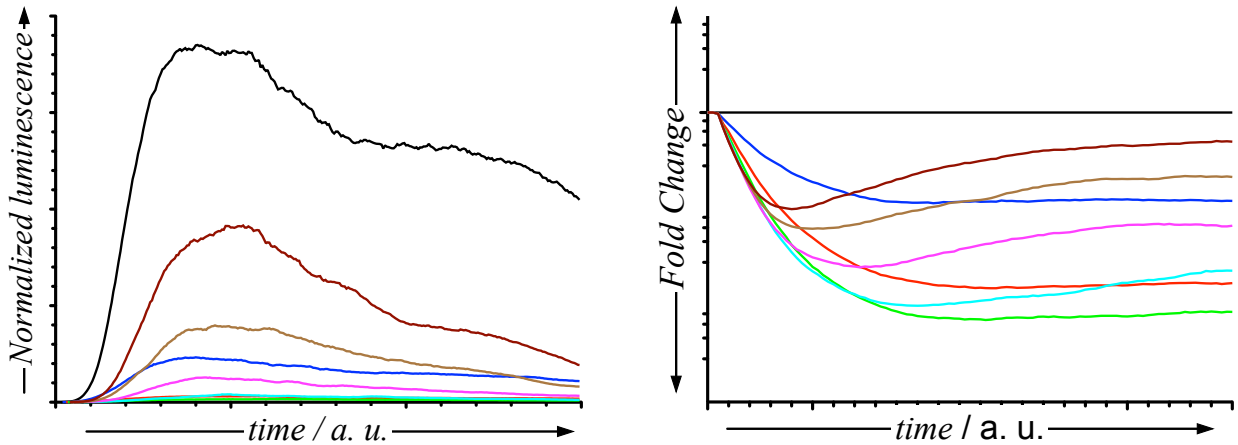

Figure S36: Predicted light production as a function of time for *V. harveyi* MM32 in the absence and presence of **P3** K_{PS} = 1, K_{PB} = 0.1 a.u. [P] = (— No polymer — 1000 — 2000 — 3000 — 4000 — 5000 — 6000 — 70000 a.u.), time = 0-3000 a.u.

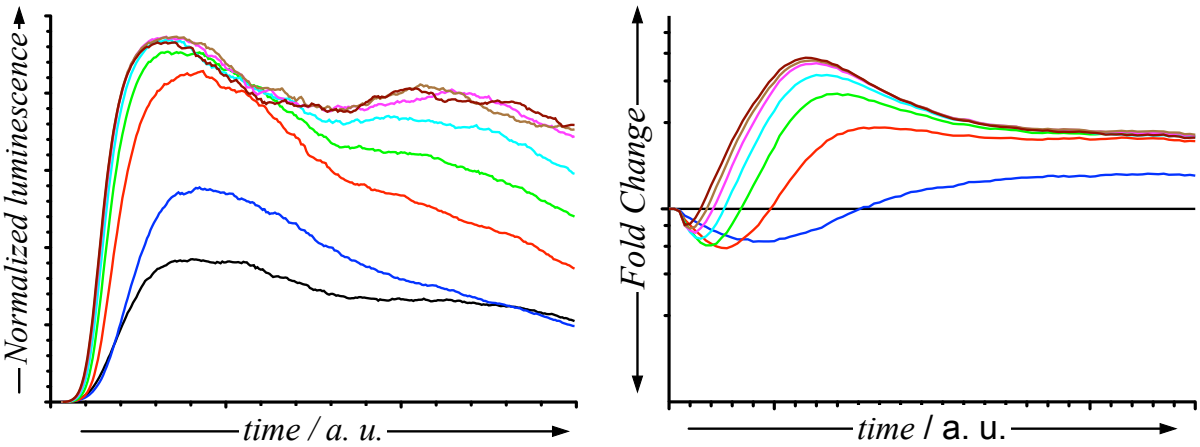

Figure S37: Predicted light production as a function of time for *V. harveyi* MM32 in the absence and presence of **P3** K_{PS} = 0.1, K_{PB} = 10 a.u. [P] = (— No polymer — 1000 — 2000 — 3000 — 4000 — 5000 — 6000 — 70000 a.u.), time = 0-3000 a.u.

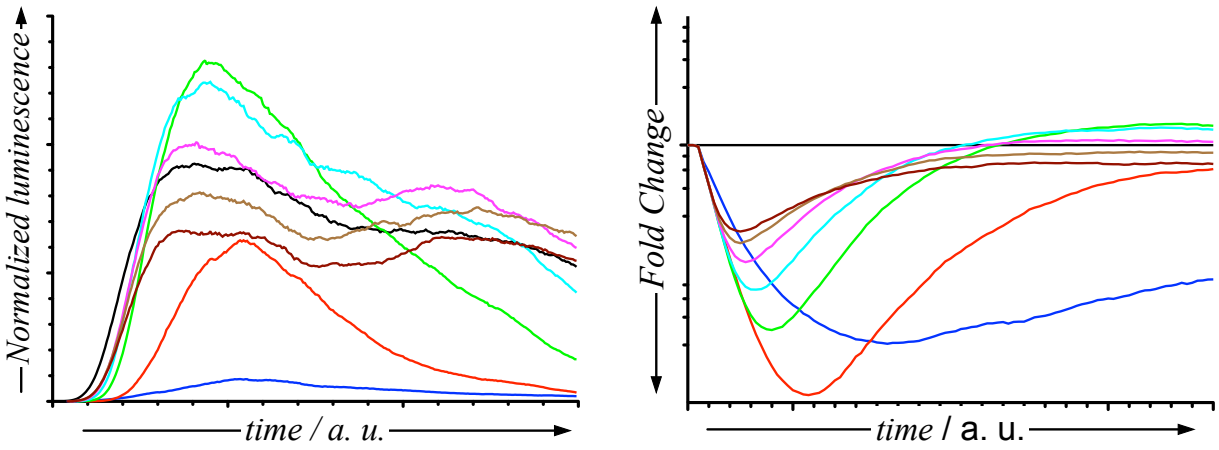

Figure S38: Predicted light production as a function of time for *V. harveyi* MM32 in the absence and presence of **P3** K_{PS} = 0.1, K_{PB} = 1 a.u. [P] = (— No polymer — 1000 — 2000 — 3000 — 4000 — 5000 — 6000 — 70000 a.u.), time = 0-3000 a.u.

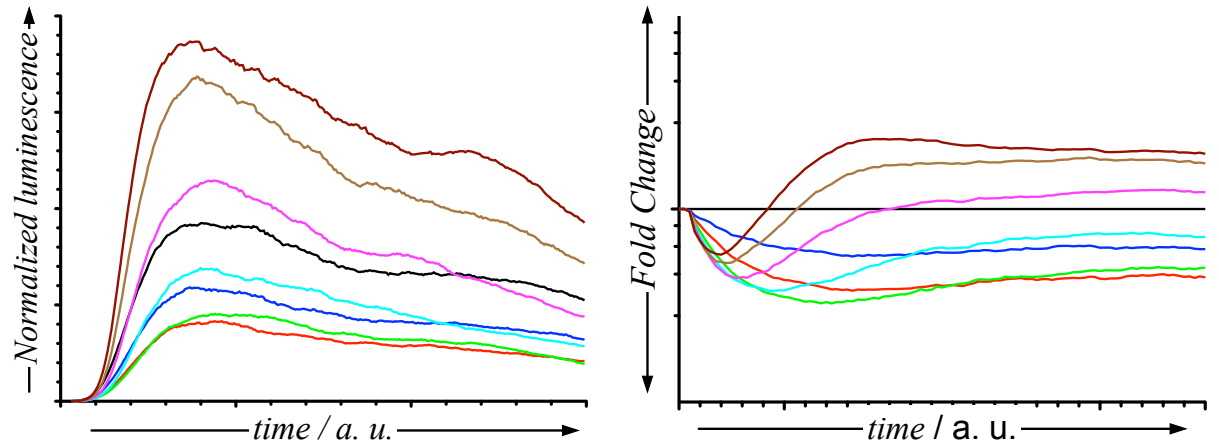

Figure S39: Predicted light production as a function of time for *V. harveyi* MM32 in the absence and presence of **P3** K_{PS} = 0.1, K_{PB} = 0.1 a.u. [P] = (— No polymer — 1000 — 2000 — 3000 — 4000 — 5000 — 6000 — 70000 a.u.), time = 0-3000 a.u.

- **Effect of cell density and growth**

The effect initial bacteria density (B_0) and growth, as controlled by doubling time (T), has on luminescence expression was investigated using BB170 and “dual-action” polymers **P3**. Polymer affinity for bacteria (K_{PB}) and signals (K_{PS}) were 5 and 10 a.u. respectively, as those reported in the main text.

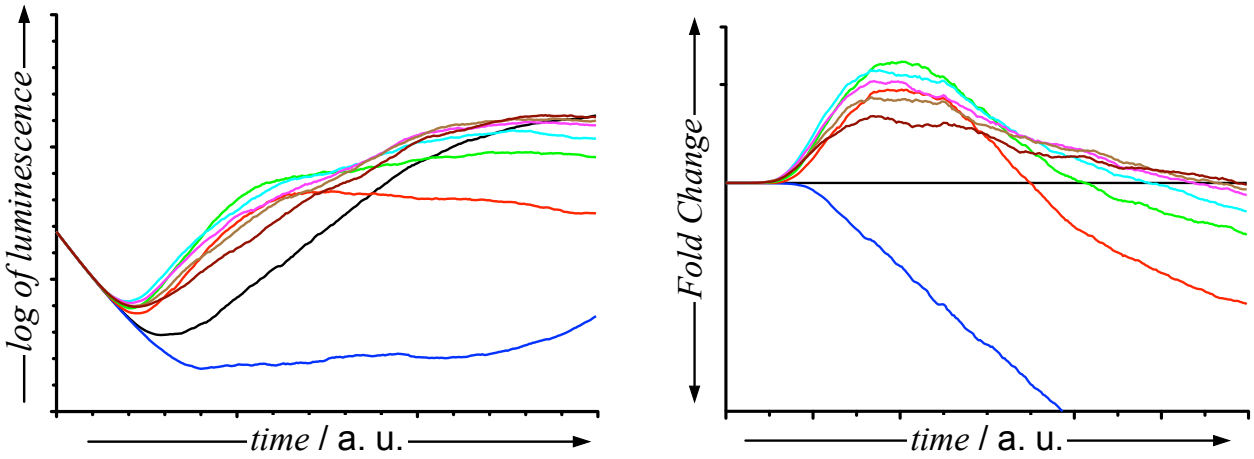

Figure S40: Predicted light production as a function of time for *V. harveyi* BB170 in the absence and presence of **P3**. B_0 = 25 a.u., T = 15000 a.u. [P] = (— No polymer — 1000 — 2000 — 3000 — 4000 — 5000 — 6000 — 70000 a.u.), time = 0-3000 a.u. (Standard conditions reported in the main text)

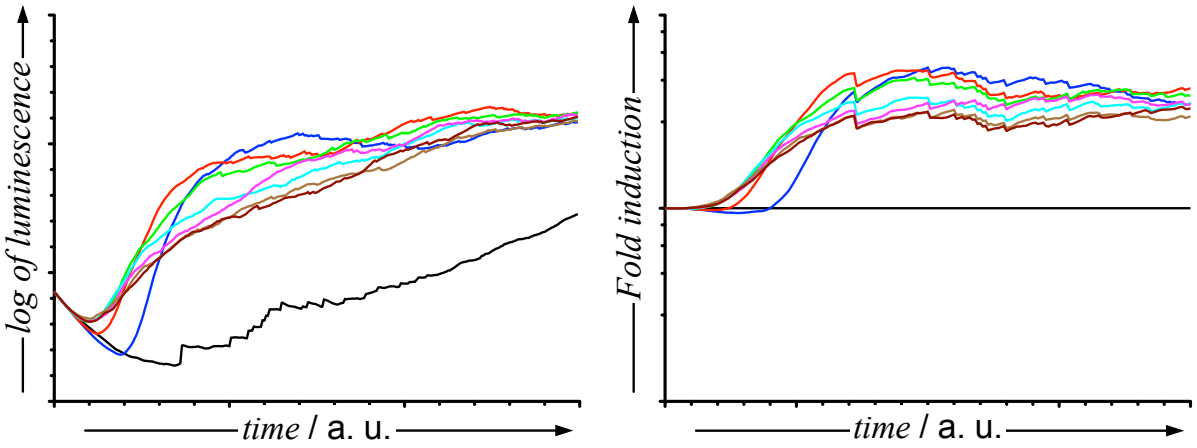

Figure S41: Predicted light production as a function of time for *V. harveyi* BB170 in the absence and presence of **P3**. B_0 = 2 a.u., T = 15000 a.u. [P] = (— No polymer — 1000 — 2000 — 3000 — 4000 — 5000 — 6000 — 70000 a.u.), time = 0-3000 a.u.

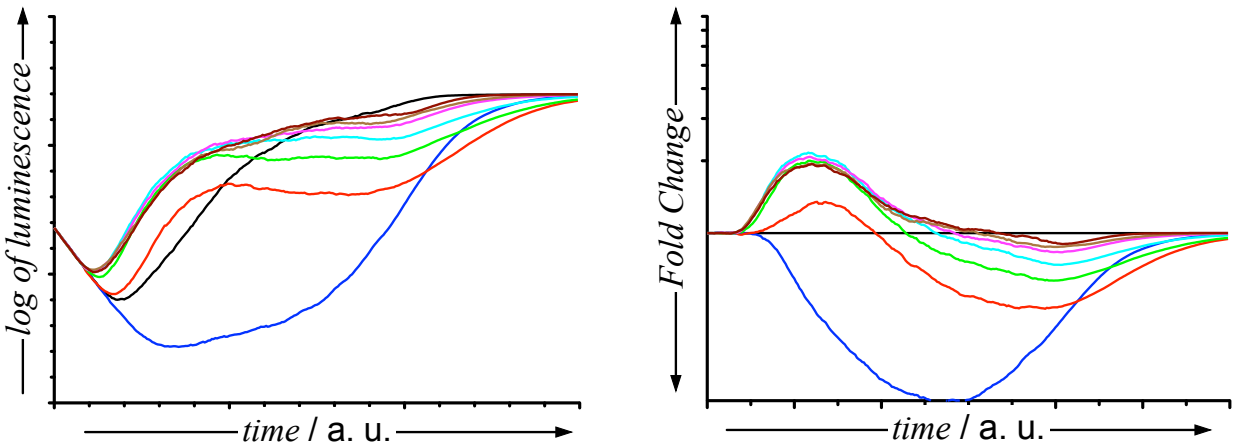

Figure S42: Predicted light production as a function of time for *V. harveyi* BB170 in the absence and presence of **P3**. B_0 = 25 a.u., T = 10000 a.u. [P] = (— No polymer — 1000 — 2000 — 3000 — 4000 — 5000 — 6000 — 70000 a.u.), time = 0-3000 a.u.

References

1. Vasilieva, Y., Thomas, D., Scales, C. & McCormick, C. Direct controlled polymerization of a cationic methacrylamido monomer in aqueous media via the RAFT p(r)ocess. *Macromolecules* **37,** 2728–2737 (2004).

2. Cooper, G. J. T. *et al.* Directed Assembly of Inorganic Polyoxometalate-based Micrometer-Scale Tubular Architectures by Using Optical Control. *Angew. Chem., Int. Ed.* **51,** 12754–12758 (2012).

3. Xue, X. et al. Synthetic Polymers for Simultaneous Bacterial Sequestration and Quorum Sense Interference. *Angew. Chem., Int. Ed*. **50**, 9852–9856 (2011).

4. Schneider, C. A., Rasband, W. S. & Eliceiri, K. W. NIH Image to ImageJ: 25 years of image analysis. *Nat. Meth*. **9**, 671–675 (2012).

5. Lorand, J. P. & Edwards, J. O. Polyol Complexes and Structure of the Benzeneboronate Ion. *J. Org. Chem*. **24**, 769–774 (1959).

6. Yan, J., Springsteen, G., Deeter, S. & Wang, B. The relationship among pK(a),pH, and binding constants in the interactions between boronic acids and diols - it is not as simple as it appears. *Tetrahedron* **60**, 11205–11209 (2003).

7. Mammen, M., Choi, S. & Whitesides, G. Polyvalent interactions in biological systems: Implications for design and use of multivalent ligands and inhibitors. *Angew. Chem., Int. Ed*. **37**, 2755–2794 (1998).

8. Simha, R. The Influence of Brownian Movement on the Viscosity of Solutions. *J. Phys. Chem*. **44**, 25–34 (1940).

9. Debye, P. The Intrinsic Viscosity of Polymer Solutions. *J. Chem. Phys*. **14**, 636 (1946).

10. Kramers, H. A. The Behavior of Macromolecules in Inhomogeneous Flow. *J. Chem. Phys*. **14**, 415 (1946).

11. Gillespie, D. T. Exact stochastic simulation of coupled chemical reactions. *J. Phys. Chem*. **81**, 2340–2361 (1977).